complete

DI-82-0043
YELLUM

D1-82-0043

BOEING SCIENTIFIC RESEARCH LABORATORIES
FLIGHT SCIENCES LABORATORY REPORT NO. 23

ANALYTICAL THEORY OF THE FLIGHT PATHS OF A GLIDER OVER A FLAT EARTH

ANGELO MIELE

JANUARY, 1960

TABLE OF CONTENTS

III

ANALYTICAL THEORY OF THE FLIGHT PATHS OF A GLIDER OVER A FLAT EARTH

by

Angelo Miele(*)

BOEING SCIENTIFIC RESEARCH LABORATORIES

SUMMARY

A general analytical theory of the flight paths of a glider operating over a flat Earth is presented. First, the equations of motion are non-dimensionalized by introducing a set of variables depending on one undetermined parameter, the reference velocity. Then, particular problems are treated, and for each of these, a convenient reference velocity is selected.

Three categories of problems are considered: (a) flight in an arbitrary atmosphere, (b) flight in a homogeneous atmosphere, and (c) flight in an exponential atmosphere. For each of these problems, a survey of previous research is made, and new analytical results are presented. Problems of type (a) are not amenable to analytical integration; on the other hand, solutions in a closed form are possible for problems of type (b)

(*)Director of Astrodynamics and Flight Mechanics

and (c) in either the low subsonic regime or the hypervelocity regime.

Analytical solutions are presented for the deceleration of a glider at constant altitude, for the class of non-steady shallow paths, and for the peak altitude reached by a sounding rocket.

The re-entry of a constant-geometry heavy missile is discussed, and an analytical determination of the points of maximum velocity and of maximum deceleration is presented. An analagous remark holds for the envelope of the largest decelerations occuring in flight.

The variable-geometry missile is also discussed. A transformation of coordinates is found which reduces the mathematical model necessary for the analysis of the variable-geometry missile to that used in the investigation of a constant-geometry missile.

Finally, attention is focused on the class of skipping paths. An analytical determination of the range flown during the skipping phase is presented, together with the analysis of the distribution of normal, tangential, and total accelerations.

LIST OF SYMBOLS

a	Speed of sound (ft sec^{-1})
C_D	Drag coefficient
C_{DO}	Drag coefficient at zero lift
C_L	Lift coefficient
D	Drag (lb)
E	Lift to drag ratio
g	Acceleration of gravity (ft sec^{-2})
h	Altitude above sea level (ft)
k	Ratio of specific heat at constant pressure to specific heat at constant volume
K	Induced drag factor
K_B	Ballistic factor
K_D	Drag factor
K_L	Lift factor
L	Lift (lb)
M	Mach number
p	Atmospherical pressure (lb ft^{-2})
R	Air constant ($ft^2 sec^{-2}\ {}^{o}R^{-1}$)
S	Reference surface for the aerodynamic coefficients (ft^2)
t	Time (sec)
u	Non-dimensional velocity
V	Flight velocity (ft sec^{-1})
V_R	Reference velocity (ft sec^{-1})

W Weight (lb)

X Horizontal distance (ft)

α Non-dimensional parameter proportional to the acceleration or to a component of the acceleration

γ Path inclination with respect to the horizon, positive for climbing

γ_E Euler's constant

ϵ Non-dimensional parameter proportional to the velocity squared

η Non-dimensional altitude

θ Absolute temperature of air ($^{\circ}R$)

λ Non-dimensional parameter, proportional to the wing loading; also, numerical constant characteristic of the exponential atmosphere (ft)

π Non-dimensional parameter proportional to the density

ρ Density (lb sec^2 ft^{-4})

σ Relative density

τ Non-dimensional time

ξ Non-dimensional horizontal distance

Superscript

Derivative with respect to non-dimensional time

Subscripts

f	Final point
i	Initial point
n	Normal acceleration
O	Either zero lift or sea level
t	Tangential acceleration

1. INTRODUCTION

In the years preceding World War II, it was a common belief among engineers that the mechanics of flight of a glider had reached a conclusive and rather stagnant stage of development. However, the progress made in the last decade has disproved this belief, mostly because of the interest aroused by the new types of hypervelocity vehicles appearing on the aeronautical horizon: ballistic missiles, glide vehicles, and skip vehicles. In this connection, a comprehensive bibliography is included (Refs. 1 through 10), although no claim of completeness is made.

In the present report, a broad, unified theory of flight trajectories for a glider operating over a flat Earth is introduced(*). Consequently, the following material is included: (a) a survey of previous research; (b) an extension of previous research (ballistic missile with constant geometry, skip vehicle); and (c) new analytical results related to several problems which, apparently, have not received

---

(*) Flight trajectories over a spherical Earth will be dealt with in a subsequent report.

sufficient attention in the aeronautical literature (deceleration at constant altitude; deceleration at variable altitude along a quasi-steady, shallow path; ascending flight of a sounding rocket; and re-entry of a ballistic missile with variable geometry).

The general method used is the following: first, the equations of motion are transformed by introducing a set of dimensionless variables which depend on one undetermined parameter, the reference velocity. Then, particular problems are treated, and for each of these, a convenient reference velocity is selected. Fixing the reference velocity is equivalent to fixing the scale by which distances, altitudes, velocities, and times are measured for each particular phenomena, as is indicated in the following analysis.

2. EQUATIONS OF MOTION

In the present report the glider is conceived as a particle operating over a flat Earth under the effect of weight, drag, and lift. The aerodynamic lag is disregarded, and the equations of motion in a vertical plane are written as follows

$$\frac{dX}{dt} - V\cos\gamma = 0 \qquad (1)$$

$$\frac{dh}{dt} - V\sin\gamma = 0 \qquad (2)$$

$$D + W\left(\sin\gamma + \frac{1}{g}\frac{dV}{dt}\right) = 0 \qquad (3)$$

$$L - W\left(\cos\gamma + \frac{V}{g}\frac{d\gamma}{dt}\right) = 0 \qquad (4)$$

where X denotes the horizontal distance traveled with respect to the Earth, h the altitude above sea level, V the velocity, γ the inclination of the flight path with respect to the horizon, D the drag, L the lift, W the weight, g the acceleration of gravity (assumed constant), and t the time.

2.1. General Integration Problem

Assuming a drag function of the form(*)

(*) This expression for the drag holds even when compressibility effects and viscosity effects are considered.

$$D = D(h, V, L)$$

the system formed by Eqs. (1) through (4) has the following features: there is one independent variable, the time, and there are five dependent variables

$$X, h, V, \gamma, L$$

Therefore, the number of degrees of freedom(*) is one, which is logical since the flight path can be changed by operating the elevator control.

Thus, for a given set of initial conditions for X, h, V, γ, an infinite number of trajectories exist which are physically and mathematically possible, more specifically, one trajectory for each arbitrarily prescribed function L(t). In view of the dissipative nature of the aerodynamic forces, no first integral can be written for the equations of motion in the general case. As a consequence, the study of particular flight conditions is of great interest from an engineering standpoint.

(*) By definition, the number of degrees of freedom of a differential system is the difference between the number of dependent variables and the number of equations.

In this report, attention is focused on some special classes of flight paths, that is, those which satisfy not only Eqs. (1) through (4) but also one additional constraint having the form

$$\Phi(t, X, h, V, \gamma, L) = 0 \qquad (5)$$

The constraining equations for several of these particular cases are as follows:

(a) For constant altitude paths

$$\Phi = h - \text{Const.} = 0 \qquad (6)$$

(b) For arbitrarily inclined rectilinear paths

$$\Phi = \gamma - \text{Const.} = 0 \qquad (7)$$

(c) For trajectories flown with constant load factor (L/W)

$$\Phi = L - \text{Const.} = 0 \qquad (8)$$

(d) For trajectories flown with constant lift coefficient

$$\Phi = \frac{L}{\rho V^2} - \text{Const.} = 0 \qquad (9)$$

where ρ is the density of the air.

2.2. Some Particular Integrals of Simplified Forms of the Equations of Motion

There are important engineering applications in which some of the terms appearing in the equations of motion are negligible with respect to the remaining terms. Consequently, it is possible to rewrite Eqs. (3) and (4) in a somewhat simplified form and obtain important analytical results, as the following analysis shows.

2.2.1. Negligible Centripetal Accelerations

If the flight path is characterized by a relatively small curvature, Eq. (4) can be replaced by

$$\frac{L}{W} - \cos\gamma = 0 \qquad (10)$$

Notice that a mathematical consequence of Eqs. (1), (2), (3), and (10) is that

$$\frac{1}{E}\frac{dX}{dt} + \frac{d}{dt}\left(h + \frac{1}{2}\frac{V^2}{g}\right) = 0$$

where E is the lift to drag ratio.

Consequently, if the trajectory is flown with constant lift to drag ratio, the following particular integral is obtained

$$\frac{X}{E} + h + \frac{1}{2}\frac{V^2}{g} = \text{Const.} \qquad (11)$$

This result is of interest for glide vehicles and is discussed further in Section 5.1.

2.2.2. Negligible Gravity Components

Another important particular case occurs when the weight is negligible with respect to the aerodynamic force. This means that Eqs. (3) and (4) become

$$D + \frac{W}{g}\frac{dV}{dt} = 0$$

$$L - W\frac{V}{g}\frac{d\gamma}{dt} = 0$$

implying that

$$\frac{dV}{V} + \frac{d\gamma}{E} = 0 \qquad (12)$$

If the lift to drag ratio is constant, one obtains

$$V \exp(\frac{\gamma}{E}) = \text{Const.} \qquad (13)$$

This result is of interest for skip vehicles and is discussed in more detail in Section 5.4.

2.3. Non-Dimensional Form of the Equations of Motion

The following non-dimensional variables are now introduced

$$\xi = X\frac{g}{V_a^2}$$

$$\eta = h\frac{g}{V_a^2} \qquad (14)$$

$$u = \frac{V}{V_R}$$

$$\tau = t \frac{g}{V_R}$$

where V_R is a constant reference speed, which is to be defined for each particular problem. Consequently, Eqs. (1) through (4) are rewritten as follows

$$\begin{aligned} \dot{\xi} - u \cos\gamma &= 0 \\ \dot{\eta} - u \sin\gamma &= 0 \\ \dot{u} + \sin\gamma + \frac{D}{W} &= 0 \\ u\dot{\gamma} + \cos\gamma - \frac{L}{W} &= 0 \end{aligned} \tag{15}$$

where the dot sign denotes derivative with respect to the non-dimensional time τ .

2.4. Aerodynamic Forces

The customary definitions of drag and lift are as follows

$$\begin{aligned} D &= \frac{1}{2} C_D \rho S V^2 \\ L &= \frac{1}{2} C_L \rho S V^2 \end{aligned} \tag{16}$$

where S is a reference surface, C_D the drag coefficient, and C_L the lift coefficient. Consequently, after introducing the reference speed V_R, the aerodynamic forces per unit weight become

$$\frac{D}{W} = \frac{C_D \rho S V_R^2}{2W} u^2$$

$$\frac{L}{W} = \frac{C_L \rho S V_R^2}{2W} u^2 \qquad (17)$$

Notice that the aerodynamic coefficients are not independent, but are related by the drag polar which can be written as

$$C_D = C_D (C_L, M) \qquad (18)$$

where M is the Mach number. While Eq. (18) applies to the entire spectrum of flight speeds, it is permissible to replace it with the following simplified form

$$C_D = C_D (C_L) \qquad (19)$$

at either low subsonic speeds or hypervelocity speeds.

An important particular case of Eq. (18) is the parabolic drag polar, which is represented by

$$C_D = C_{DO} + K C_L^2 \qquad (20)$$

where

$$C_{DO} = C_{DO}(M) \ , \ K = K(M)$$

in the entire spectrum of flight speeds. However, these functions can be replaced by constants in either the low subsonic regime or the hypervelocity regime.

2.5. Remark

In the following sections several physical problems are analyzed, and for each of these, a convenient reference speed is introduced. Clearly, fixing the reference velocity is equivalent to fixing the scale by which distances, altitudes, velocities, and times are measured. At any rate, the general criterion followed in the choice of V_R is that of reducing Eqs. (15) to the simplest form suitable for analytical purposes.

3. ARBITRARY ATMOSPHERE

The most general problem of the Mechanics of Flight of a glider occurs when the distribution of the atmospheric properties versus the altitude is arbitrarily specified and the drag polar satisfies Eq. (18).

For such a case, which is of interest at high subsonic, transonic, and supersonic speeds, it is convenient to assume the following reference velocity

$$V_R = a_o = \sqrt{kR\theta_o}$$

where a_o is the speed of sound at sea level, R the air constant, and θ_o the static temperature at sea level. Consequently, the equations of motion are rewritten as follows

$$\begin{aligned} \dot{\xi} - u\cos\gamma &= 0 \\ \dot{\eta} - u\sin\gamma &= 0 \\ \dot{u} + \sin\gamma + \frac{C_D\sigma u^2}{\lambda} &= 0 \\ u\dot{\gamma} + \cos\gamma - \frac{C_L\sigma u^2}{\lambda} &= 0 \end{aligned} \qquad (21)$$

where σ is the relative density of air, and

$$\lambda = \frac{2W}{kp_o S} \qquad (22)$$

is a non-dimensional parameter proportional to the wing loading. The symbol p_o denotes the atmospheric pressure at sea level. Notice that the integration of Eqs. (21)

is to be carried out subject to Eq. (18) and to the following relationship between the Mach number and the non-dimensional speed

$$M = \frac{u}{A} = \frac{u}{\sqrt{T}} \tag{23}$$

where

$$A = \frac{a}{a_*}$$

$$T = \frac{\theta}{\theta_*}$$

3.1. Rectilinear Paths

If the aircraft moves along an arbitrarily inclined, rectilinear path, the constraint (7) is to be considered; consequently, the equation of motion on the normal to the flight path reduces to

$$C_L = \frac{\lambda \cos\gamma}{\sigma u^2} \tag{24}$$

This means that, for the particular case of a parabolic drag polar, the dynamical relationships and the kinematic relationship on the vertical direction lead to

$$\frac{du}{d\eta} + \frac{1}{u} + \frac{1}{\sin\gamma}\left[\frac{C_{DO}\sigma u}{\lambda} + \frac{K\lambda}{\sigma u^3}\cos^2\gamma\right] = 0 \tag{25}$$

where the coefficients C_{DO} and K, which depend upon the Mach number, can be rewritten as

$$C_{D_0} = C_{D_0}\left(\frac{u}{\sqrt{T}}\right)$$

$$K = K\left(\frac{u}{\sqrt{T}}\right)$$

Consequently, it is concluded that the integration of Eq. (25) alone yields the velocity-altitude distribution. The time, in turn, can be found a posteriori by employing the following differential equation

$$d\tau = \frac{d\eta}{u \sin\gamma}$$

For the particular case of a vertical path, Eq. (25) reduces to

$$\frac{du}{d\eta} + \frac{1}{u} \pm \frac{C_{D_0}\sigma u}{\lambda} = 0 \qquad (26)$$

the positive sign applying to ascending flight and the negative sign to descending flight.

3.2. Alternative Formulation

An alternative formulation of the equations of motion can be obtained by carrying out the elimination of the non-dimensional speed from Eqs. (21). Simple manipulations, omitted for the sake of brevity, lead to

$$\dot{\xi} - M A \cos\gamma = 0$$

$$\dot{\eta} - M A \sin\gamma = 0$$

$$\dot{M} A + \left[1 + \frac{M^2}{2} \frac{dT}{d\eta} \right] \sin\gamma + \frac{C_D M^2 P}{\lambda} = 0$$

$$M A \dot{\gamma} + \cos\gamma - \frac{C_L M^2 P}{\lambda} = 0$$

where

$$P = \frac{p}{p_o}$$

As an example, for the particular case of a rectilinear path, these equations imply that

$$\frac{dM^2}{d\eta} + \frac{2}{T} \left[1 + \frac{M^2}{2} \frac{dT}{d\eta} \right] +$$

$$+ \frac{2}{T \sin\gamma} \left[\frac{C_{Do} M^2 P}{\lambda} + \frac{K \lambda \cos^2\gamma}{M^2 P} \right] = 0$$

3.3. Remark

The general problem formulated in the previous section and the particular example of rectilinear flight indicate that the equations describing the behavior of a glider at high subsonic, transonic, and supersonic speeds in an arbitrary atmosphere are not amenable to analytical integration. However, closed form solutions

are possible for some particular distributions of the atmospheric properties versus the altitude and for some particular flow regimes. These solutions, which are of great interest in engineering, are discussed in the following sections.

4. HOMOGENEOUS ATMOSPHERE

If the altitude variation is sufficiently small, the density of the air can be regarded as a constant. Consequently, it is natural to assume the following reference speed

$$V_R = \sqrt{\frac{2W}{\rho S}}$$

so that the equations of motion can be written as

$$\begin{aligned} \dot{\xi} - u\cos\gamma &= 0 \\ \dot{\eta} - u\sin\gamma &= 0 \\ \dot{u} + \sin\gamma + C_D u^2 &= 0 \\ u\dot{\gamma} + \cos\gamma - C_L u^2 &= 0 \end{aligned} \tag{27}$$

4.1. Constant Aerodynamic Coefficients

If the coefficients of lift and/or drag are kept constant during flight, either of the following reference speeds is of interest

$$V_R = \sqrt{\frac{2W}{C_L \rho S}} \tag{28}$$

$$V_R = \sqrt{\frac{2W}{C_D \rho S}} \tag{29}$$

If reference speed (28) is used, the equations of motion take thefollowing form

$$\begin{aligned} \dot{\xi} - u\cos\gamma &= 0 \\ \dot{\eta} - u\sin\gamma &= 0 \\ \dot{u} + \sin\gamma + \frac{u^2}{E} &= 0 \\ u\dot{\gamma} + \cos\gamma - u^2 &= 0 \end{aligned} \tag{30}$$

where E is the lift to drag ratio.

On the other hand, if reference speed (29) is used, the motion of the aircraft is described by

$$\begin{aligned} \dot{\xi} - u\cos\gamma &= 0 \\ \dot{\eta} - u\sin\gamma &= 0 \\ \dot{u} + \sin\gamma + u^2 &= 0 \\ u\dot{\gamma} + \cos\gamma - E\,u^2 &= 0 \end{aligned} \tag{31}$$

4.2. Non-Lifting Paths(*)

A flight path flown at zero lift in a constant density medium is now considered. Assuming that the drag coefficient is constant, Eq. (31-4) modifies as follows

---

(*) This problem is of interest for objects launched at subsonic speeds and low altitudes and has been previously studied by Templin and Callan (Ref. 6).

$$\dot{\gamma} + \frac{\cos\gamma}{u} = 0 \qquad (32)$$

Elimination of the time from Eqs. (31-3) and (32) leads to the following expression

$$\frac{du}{d\gamma} - u\tan\gamma - \frac{u^3}{\cos\gamma} = 0$$

which can be rewritten as

$$\frac{d\psi}{\psi^3} - \frac{d\gamma}{\cos^3\gamma} = 0 \qquad (33)$$

where

$$\psi = u\cos\gamma$$

is the velocity component in the horizontal direction. The general solution for this differential equation is

$$\frac{1}{\psi^2} + \frac{\sin\gamma}{\cos^2\gamma} + \log\tan\left|\frac{\pi}{4} + \frac{\gamma}{2}\right| = C$$

that is

$$u = \frac{1}{\sqrt{\left[C - \log\tan\left|\frac{\pi}{4} + \frac{\gamma}{2}\right|\right]\cos^2\gamma - \sin\gamma}} \qquad (34)$$

where C is a constant. The above relation is plotted in Fig. 1 for several values of the integration constant C.

Notice that the velocity has a minimum for the following value of the path inclination

$$\gamma = -\arcsin u^2$$

Furthermore, there is the asymptotic value for the path inclination, which is defined by (Fig. 2)

$$C = \frac{\sin\gamma}{\cos^2\gamma} + \log \tan \left| \frac{\pi}{4} + \frac{\gamma}{2} \right|$$

Once the distribution of velocity is known, the geometry of the trajectory and the time can be determined a posteriori by using the following relationships

$$\begin{aligned} \frac{d\xi}{d\gamma} &= - u^2 \\ \frac{d\eta}{d\gamma} &= - u^2 \tan\gamma \\ \frac{d\tau}{d\gamma} &= - \frac{u}{\cos\gamma} \end{aligned} \qquad (35)$$

In this connection, assuming $\xi_1 = \gamma_1 = 0$, Fig. 3 indicates the trajectory followed by the vehicle for several values of the initial velocity. The latter is related to the integration constant C by the relationship

$$u_1 = \frac{1}{\sqrt{C}}$$

The asymptotic range $\xi_{\pi/2}$, reached when the flight path becomes vertical, is indicated in Fig. 4 as related to the initial velocity u_1.

4.3. Vertical Paths

For the particular case of vertical flight Eqs. (31-2) and (31-3) reduce to

$$\dot{\eta} \mp u = 0$$

$$\dot{u} \pm 1 + u^2 = 0$$

the upper sign corresponding to ascending paths and the lower sign to descending paths. These equations can be rewritten as

$$d\tau = \mp \frac{du}{1 \pm u^2}$$

$$d\eta = -\frac{1}{2} \frac{du^2}{1 \pm u^2}$$

and admit the following solutions

(a) For ascending flight

$$\tau = -\arctan u + \text{Const.}$$

$$\eta = -\frac{1}{2} \log (1 + u^2) + \text{Const.}$$

(b) For descending flight

$$\tau = \frac{1}{2} \log \left| \frac{1 + u}{1 - u} \right| + \text{Const.}$$

$$\eta = \frac{1}{2} \log \left| 1 - u^2 \right| + \text{Const.}$$

4.4. Constant Altitude. Parabolic Polar with Constant Coefficients.

For constant altitude flight the constraint

$$\eta - \text{Const.} = 0$$

must be considered, so that $\gamma = 0$. If the drag polar satisfies Eq. (20) and if C_{D0} and K are constant, then the following reference velocity is of interest

$$V_R = \sqrt{\frac{2W}{\rho S}} \quad \sqrt[4]{\frac{K}{C_{D0}}}$$

After simple manipulations, the equations of motion become

$$\dot{\xi} - u = 0 \tag{36}$$

$$\dot{u} + \frac{1}{2E_{max}} \left[u^2 + \frac{1}{u^2} \right] = 0 \tag{37}$$

$$C_L u^2 \sqrt{\frac{K}{C_{D0}}} - 1 = 0 \tag{38}$$

where

$$E_{max} = \frac{1}{2\sqrt{KC_{D0}}}$$

is the maximum value of the lift to drag ratio.

It is apparent from Eq. (38) that the product

$$C_L u^2$$

is constant along the flight path. This means that, owing to the progressive decrease in the flight speed, the angle of attack must be continuously increased in order to satisfy the condition of dynamic equilibrium on

the normal to the flight path. Furthermore, Eqs. (36) and (37) lead to the following differential equations

$$\frac{d\xi}{E_{max}} = - \frac{2u^3}{1+u^4}\, du$$

$$\frac{d\tau}{E_{max}} = - \frac{2u^2}{1+u^4}\, du$$

whose integration yields

$$\frac{\xi}{E_{max}} = - A(u) + \text{Const.} \qquad (39)$$

$$\frac{\tau}{E_{max}} = - B(u) + \text{Const.} \qquad (40)$$

where A and B are functions of the non-dimen.ional speed defined by (Fig. 5)

$$A(u) = \frac{1}{2} \log (1+u^4) \qquad (41)$$

$$B(u) = \frac{1}{\sqrt{2}} \left[\arctan \frac{u\sqrt{2}}{1-u^2} - \frac{1}{2} \log \frac{1+u^2+u\sqrt{2}}{1+u^2-u\sqrt{2}} \right] \qquad (42)$$

This means that, if a glider is decelerated at constant altitude between an initial speed u_i and a final speed u_f, the distance and the time are given by

$$X_f - X_i = \frac{V_R^2 E_{max}}{g} \left[A(u_i) - A(u_f) \right] \qquad (43)$$

$$t_f - t_i = \frac{V_R E_{max}}{g} \left[B(u_i) - B(u_f) \right] \qquad (44)$$

These two quantities are plotted in Fig. 6 for a typical jet transport ($W/S = 60$ lb ft^{-2}, $C_{D_0} = 0.015$, $K = 0.042$) and for the following end-conditions

$$V_1 = 750 \text{ ft sec}^{-1}, \quad V_f = 300 \text{ ft sec}^{-1}$$

The graph indicates that both the distance and the time increase with the altitude. For example, the distance covered by the aircraft while gliding is about 15 miles at sea level and about 24 miles at 30,000 ft.

5. EXPONENTIAL ATMOSPHERE

There are many engineering problems in which important qualitative conclusions can be reached by assuming an exponential law for the density-altitude relationship, that is

$$\sigma = \exp\left(-\frac{h}{\lambda}\right)$$

where λ is a dimensional constant [*] [**]. If the following reference velocity is considered

$$V_R = \sqrt{\lambda g}$$

the density-altitude relationship can be rewritten as

$$\sigma = \exp(-\eta)$$

---

[*] The suggested value for the constant λ in the altitude interval 0-250,000 ft is

$$\lambda = 23{,}200 \text{ ft}$$

[**] A particular case of the exponential atmosphere is the isothermal atmosphere. For this case, the fundamental constant becomes

$$\lambda = \frac{a^2}{kg}$$

where a is the speed of sound and k the ratio of the specific heat at constant pressure to the specific heat at constant volume. Consequently, the non-dimensional speed and the Mach number are related by

$$u = M\sqrt{k}$$

Consequently, the equations of motion take the following form

$$\begin{aligned} \dot{\xi} - u\cos\gamma &= 0 \\ \dot{\sigma} + u\sigma\sin\gamma &= 0 \\ \dot{u} + \sin\gamma + K_D u^2\sigma &= 0 \\ u\dot{\gamma} + \cos\gamma - K_L u^2\sigma &= 0 \end{aligned} \tag{45}$$

where K_D and K_L are non-dimensional quantities defined by

$$K_D = \frac{C_D \rho_0 S \lambda R}{2W} \tag{46}$$

$$K_L = \frac{C_L \rho_0 S \lambda R}{2W} \tag{47}$$

and called, respectively, the drag factor and the lift factor.

In the following sections, the integration of Eqs. (45) is discussed for several particular cases, that is: (a) trajectories flown with negligible centripetal acceleration and small inclination with respect to the horizon, (b) vertically ascending paths, (c) re-entry paths, and (d) skipping paths.

5.1. Negligible Centripetal Acceleration. Small Inclinations with Respect to the Horizon.

If the curvature of the flight path is relatively small and if its inclination with respect to the horizon is small, the equations of motion simplify as follows

$$\begin{aligned} \dot{\xi} - u &= 0 \\ \dot{\sigma} + u\sigma\gamma &= 0 \\ \dot{u} + \gamma + K_D u^2 \sigma &= 0 \\ K_L u^2 \sigma - 1 &= 0 \end{aligned} \tag{48}$$

Consider, now, the particular case of either low subsonic flight or hypervelocity flight, and assume that the aerodynamic coefficients depend only on the angle of attack. Assume, also, that the angle of attack is maintained constant along the flight path so that K_L, K_D, E are simultaneously constant.

After simple manipulations, omitted for the sake of brevity, all the variables of the problem can be expressed in terms of the instantaneous velocity. Thus, the relative density is given by

$$\sigma = \frac{1}{K_L u^2}$$

and implies the following result

$$\eta = \log K_L + 2 \log u \tag{49}$$

which is plotted in Fig. 7 for the low subsonic regime. Furthermore, the instantaneous inclination of the flight path is

$$\gamma = -\frac{1}{E}\frac{2}{2+u^2} \tag{50}$$

and is plotted in Fig. 8 for the low subsonic regime. As Eq. (50) shows, the altitude decreases continuously along the flight path. Consequently, it is seen from Eq. (49) that the velocity also decreases.

The differential equations for the distance and the time become

$$\frac{d\xi}{E} + \left(\frac{2}{u} + u\right) du = 0$$

$$\frac{d\tau}{E} + \left(\frac{2}{u^2} + 1\right) du = 0$$

and can be integrated to give

$$\frac{\xi}{E} = \alpha(u) + \text{Const.} \tag{51}$$

$$\frac{\tau}{E} = \beta(u) + \text{Const.} \tag{52}$$

where the functions $\alpha(u)$ and $\beta(u)$ are defined as

$$\alpha(u) = -\left(2 \log u + \frac{u^2}{2}\right)$$

$$\beta(u) = \frac{2}{u} - u$$

and are plotted in Fig. 9 for the low subsonic regime.

Notice that a mathematical consequence of Eqs. (49) and (51) is the following expression

$$\frac{\xi}{E} + \eta + \frac{u^2}{2} = \text{Const.} \qquad (53)$$

which is the dimensionless form of Eq. (11). Notice, also, that Eqs. (48-4) and (52) lead to the important result

$$\frac{\tau}{E} - 2\sqrt{K_L \sigma} + u = \text{Const.} \qquad (54)$$

5.1.1. Discussion

Consider a trajectory flown between a given initial condition (subscript i) and a given final condition (subscript f), and rewrite the above two equations in the form

$$\xi_f - \xi_i = E\left(\eta_i - \eta_f + \frac{u_i^2 - u_f^2}{2}\right) \qquad (55)$$

$$\tau_f - \tau_i = 2E\sqrt{K_L}\,(\sqrt{\sigma_f} - \sqrt{\sigma_i}) + E(u_i - u_f) \qquad (56)$$

Eq. (55) clearly shows that the glider is capable of converting potential and kinetic energy into the work necessary to achieve range in a resisting medium. Since the transformation factor is the lift to drag ratio, it is concluded that: (a) the lift to drag ratio is an

important item in the aerodynamic design of gliders and (b) the best range is achieved by flying at the angle of attack which maximizes the lift to drag ratio.

5.1.2. Quasi-Steady Solution

If the variation in kinetic energy is small with respect to the variation in potential energy, then the previous equations simplify into (*)

$$\xi_f - \xi_i = E(\eta_i - \eta_f)$$

$$\tau_f - \tau_i = 2E\sqrt{K_L}\,(\sqrt{\sigma_f} - \sqrt{\sigma_i})$$

Consequently, the range is proportional to the lift to drag ratio, while the time is proportional to $E\sqrt{C_L}$. This means that the condition of flattest descent and that of slowest descent are achieved by flying at two different angles of attack. More specifically, the flattest descent requires a lower angle of attack, and consequently, a higher flight velocity than the slowest descent.

(*) This approximation is equivalent to neglecting the term $\frac{W}{g}\frac{dV}{dt}$ in Eq. (3).

5.1.3. Hypervelocity Solution

If the variation in potential energy is small with respect to the variation in kinetic energy, then Eqs. (55) and (56) simplify into(*)

$$\xi_f - \xi_i = \frac{E}{2}(u_i^2 - u_f^2)$$

$$\tau_f - \tau_i = E(u_i - u_f)$$

These equations are a special case of those derived by Eggers-Allen-Neice and by Sänger-Bredt for flight over a spherical Earth and can be obtained from those of Refs. 2 and 10 by means of the limiting process $r_o \longrightarrow \infty$(**).

5.2. Vertically Ascending Paths

A trajectory of interest for sounding rockets is the vertically ascending path. For $\gamma = \pi/2$, Eqs. (45) simplify as follows

$$\begin{aligned} \dot{\xi} &= 0 \\ \dot{\sigma} + u\sigma &= 0 \\ \dot{u} + 1 + K_D u^2 \sigma &= 0 \\ K_t &= 0 \end{aligned} \qquad (57)$$

(*) This approximation is equivalent to neglecting the term $W \sin\gamma$ in Eq. (3).

(**) The symbol r_o denotes the radius of the Earth.

and imply that

$$\frac{du}{d\sigma} - K_D u - \frac{1}{u\sigma} = 0$$

where K_D is the drag factor evaluated at zero lift.

Introducing the following new variables

$$\pi = 2 K_D \sigma$$

$$\epsilon = \frac{u^2}{2}$$

and assuming a constant drag factor, one obtains

$$\frac{d\epsilon}{d\pi} - \epsilon - \frac{1}{\pi} = 0 \qquad (58)$$

The general solution for this differential equation is

$$\epsilon = \left[C + Ei(-\pi) \right] \exp(\pi) \qquad (59)$$

where the exponential-integral function is defined by

$$Ei(-\pi) = \int_{\infty}^{\pi} \frac{e^{-t}}{t} \, dt \qquad (60)$$

and is tabulated in Ref. 5. Notice that this function can be expanded as

$$Ei(-\pi) = \gamma_E + \log \pi + \sum_{n=1}^{\infty} \frac{(-\pi)^n}{n \, ! \, n}$$

where

$$\gamma_E = 0.5772$$

is Euler's constant and where

$$\log \pi = \log(2K_D) - \eta$$

Consider, now, the problem of determining the peak altitude reached by a sounding rocket for a given initial velocity and a given initial altitude. After determining the constant C in terms of both the initial and final conditions ($u_f = 0$), the following implicit solution is obtained

$$Ei(-\pi_f) - Ei(-\pi_i) + \frac{u_i^2}{2} \exp(-\pi_i) = 0 \qquad (61)$$

If the conditions at the final point are such that

$$\pi_f << 1$$

the final altitude can be approximated by

$$\eta_f = \gamma_E + \log(2K_D) - Ei(-\pi_i) + \frac{u_i^2}{2} \exp(-\pi_i)$$

which reduces to

$$\eta_f = \eta_i + \frac{u_i^2}{2}$$

for flight in a vacuum. This is logical, since the sum of the potential energy and the kinetic energy must be constant if no dissipative effect is present.

The result indicated in Eq. (61) is plotted in Figs. 10 and 11. Fig. 10 shows the peak altitude versus the initial velocity for $\eta_i = 0$ and for several values of the drag factor, while Fig. 11 shows the peak altitude versus the initial velocity for $K_D = 0.1$ and several values of the initial altitude.

As Fig. 10 indicates, for a sounding rocket whose drag factor is $K_D = 0.1$, the peak altitude is about 80% of that which would be obtained in a vacuum. On the other hand, for $K_D = 1$ the peak altitude becomes about 15% of that corresponding to flight in a vacuum. As a conclusion, a low value of the drag factor is of fundamental importance in the correct design of high-performance sounding rockets.

Remark. The engineering data presented in this section must be taken cum grano salis owing to the fact that the variability of the acceleration of gravity with the altitude has been disregarded.

5.3. Re-Entry Paths(*)

The re-entry of a ballistic missile is now considered under the assumption that the angle of attack and, therefore, the lift coefficient is zero everywhere. For $K_L = 0$, Eqs. (45) are rewritten as follows

---

(*) This problem has been previously investigated by Allen and Eggers (Ref. 1) and extended in Refs. 3, 6, 8, and 9. The new contribution presented here is concerned with the analytical determination of: (a) the point of maximum velocity, (b) the point of maximum deceleration, and (c) the envelope of the largest decelerations of a heavy missile.

$$\frac{d\xi}{d\sigma} + \frac{\cot\gamma}{\sigma} = 0$$

$$\frac{d\tau}{d\sigma} + \frac{1}{u\sigma\sin\gamma} = 0$$

$$\frac{du}{d\sigma} - \frac{K_D}{\sin\gamma}u - \frac{1}{u\sigma} = 0 \qquad (62)$$

$$\frac{d\gamma}{d\sigma} - \frac{\cot\gamma}{\sigma u^2} = 0$$

The last of these equations shows that the overall variation in the slope of the flight path during re-entry is tied to the average value of $\cot\gamma/\sigma u^2$. If the flight path is rather steep with respect to the horizon and if $u^2 >> 1$, then the overall variation in the slope is small. As a consequence, the trigonometric functions appearing in Eqs. (62) can be approximated by their values at the initial point. This simplifies the integration problems considerably, insofar as Eq. (62-3) yields the velocity-altitude distribution; the other three equations are employed a posteriori in order to predict the range, the time, and the inclination of the flight path.

Since the path inclination is negative, it is convenient to define the following parameter

$$K_B = -\frac{2K_D}{\sin\gamma_1}$$

which is called the ballistic factor. As a consequence,

after introducing the non-dimensional variables(*)

$$\pi = K_0 \sigma \tag{63}$$

$$\epsilon = \frac{u^2}{2} \tag{64}$$

Eq. (62-3) is rewritten as

$$\frac{d\epsilon}{d\pi} + \epsilon - \frac{1}{\pi} = 0 \tag{65}$$

and admits the following general solution

$$\epsilon = \left[C + Ei(\pi) \right] \exp(-\pi) \tag{66}$$

where C is a constant. The exponential-integral function appearing in this equation is defined by (Ref. 5)

$$Ei(\pi) = \int_{-\infty}^{\pi} \frac{e^t}{t} \, dt \tag{67}$$

and can be expanded as

$$Ei(\pi) = \gamma_E + \log \pi + \sum_{n=1}^{\infty} \frac{\pi^n}{n \, ! \, n}$$

(*) The variable π is proportional to the drag per unit weight component on the tangent to the flight path calculated at $u = 1$; the variable ϵ is proportional to the kinetic energy of the missile per unit mass.

The constant C can be determined from the known initial conditions. If initial altitudes in the order of 200,000 ft. or more are considered, Eq. (66) yields the following approximate result

$$C = \frac{u_1^2}{2} + \eta_1 - \gamma_1 - \log K_1 \qquad (68)$$

Notice that, for the re-entry conditions characteristic of intermediate range and long range missiles, the predominant term in the right-hand side of Eq. (68) is the kinetic energy term. Consequently, the constant C is approximately equal to the non-dimensional kinetic energy of the missile at the initial point. Typical values are C = 100 for intermediate range missiles and C = 300 for long range missiles.

Velocity. Because of Eqs. (64) and (66), the distribution of velocities along a re-entry path is given by

$$u = \sqrt{2\left[C + \mathrm{Ei}(\pi)\right]\exp(-\pi)} \qquad (69)$$

and is plotted in Figs. 12 and 13 for two values of the integration constant C. Notice that the ordinate is $u/\sqrt{2C}$, since this parameter is approximately equal to the ratio of velocity to initial velocity for most re-entry paths.

As Fig. 12 indicates, the velocity diagram has a maximum at the altitude where (Fig. 14)

$$C = \frac{\exp(\pi)}{\pi} - Ei(\pi) \qquad (70)$$

Such a maximum can be calculated by substituting the value of π which satisfies Eq. (70) into either Eq. (69) or

$$u = \sqrt{\frac{2}{\pi}} \qquad (71)$$

and is plotted in Fig. 15. Physically, the existence of a maximum for the velocity is due to the fact that in the initial part of a re-entry trajectory the weight of the missile is predominant with respect to the aerodynamic drag, whereas this condition is reversed at lower altitudes.

Deceleration. In order to study the deceleration of a ballistic missile, it is convenient to define the following dimensionless parameter

$$\alpha = \frac{1}{g \sin\gamma_1} \frac{dV}{dt} \qquad (72)$$

and observe that, because of the equations of motion,

$$\alpha = \epsilon \pi - 1$$

which implies that

$$\alpha = \pi \left[C + Ei(\pi) \right] \exp(-\pi) - 1 \qquad (73)$$

The function α/C is plotted in Fig. 16 for $C = 100$ and $C = 300$ and is roughly independent of C in the range

of values of the constant which are characteristic of intermediate range and long range missiles. In consideration of Eq. (68), it is concluded that the deceleration α increases, approximately, as the square of the entrance velocity.

Incidentally, the deceleration has a maximum at the altitude where (Fig. 17)

$$C = \frac{\exp(\pi)}{\pi - 1} - \mathrm{Ei}(\pi) \tag{74}$$

Such a maximum can be calculated by substituting the value of π which satisfies Eq. (74) into either Eq. (73) or

$$\alpha = \frac{1}{\pi - 1} \tag{75}$$

and is plotted in Fig. 18.

Furthermore, the maximum occurs above sea level if, and only if, the following inequality is satisfied

$$C - \frac{\exp(K_s)}{K_s - 1} + \mathrm{Ei}(K_s) > 0 \tag{76}$$

If the missile configuration and the initial conditions are not consistent with the inequality (76), then the highest deceleration (not an analytical maximum) occurs at sea level and is given by

$$\alpha = K_s \left[C + \mathrm{Ei}(K_s) \right] \exp(-K_s) - 1 \tag{77}$$

The results indicated by expressions (74) through (77) are plotted in Fig. 19, which supplies the envelope of the largest decelerations occuring in the re-entry of a constant geometry missile. The dot-dash line of Fig. 19 splits the ballistic factor-deceleration domain into two regions: the region on the right of this line corresponds to the occurrence of an analytical maximum above sea level; the region on the left corresponds to the occurrence of the highest deceleration (not an analytical maximum) at sea level.

5.3.1. Light Body Approximation

An approximate analysis of the re-entry of a ballistic missile can be developed under the assumption that the gravitational forces are negligible with respect to the aerodynamic forces. In this case, the trajectory becomes a straight line along which the variation in kinetic energy is given by

$$\frac{d\epsilon}{d\pi} + \epsilon = 0$$

The general solution for this differential equation is

$$\epsilon = C \exp(-\pi) \tag{78}$$

where

$$C \simeq \frac{u_1^2}{2} \tag{79}$$

if initial altitudes in the order of 200,000 ft. or more are considered.

Velocity. Because of Eqs. (64) and (78), the velocity distribution is given by (Figs. 12 and 13)

$$\frac{u}{\sqrt{2C}} = \exp(-\frac{\pi}{2}) \tag{80}$$

which implies that

$$\frac{u}{\sqrt{2C}} = \exp\left[-\frac{K_B}{2}\exp(-\eta)\right] \tag{81}$$

This function is plotted in Fig. 20 for several values of the ballistic factor. As the diagram indicates, values of $K_B < 0.1$ yield re-entry paths characterized by velocity drops of less than 5% of the initial velocity. On the other hand, for $K_B > 1$ a considerable decrease in velocity occurs during re-entry; this means that a large fraction of the kinetic energy of the missile is expended in generating and maintaining the aerodynamic field around the body.

Deceleration. Under the light body approximation, the instantaneous deceleration is given by (Fig. 16)

$$\frac{\alpha}{C} = \pi \exp(-\pi) \tag{82}$$

which implies that

$$\frac{\alpha}{C} = K_B \exp(-\eta)\exp[-K_B\exp(-\eta)] \tag{83}$$

This relation is plotted in Fig. 21 for several values of the ballistic factor. As the diagram indicates, any value of $K_s > 1$ yields an analytical maximum for the deceleration at some altitude above sea level. Such a maximum occurs at

$$\pi = 1$$

and is supplied by

$$\frac{\alpha}{C} = \frac{1}{e} \tag{84}$$

In the case where the missile configuration is such that

$$K_s < 1$$

the largest value of the deceleration (not an analytical maximum) occurs at sea level and is given by

$$\frac{\alpha}{C} = K_s \exp(-K_s) \tag{85}$$

Remark. The previous diagrams permit an interesting comparison between the re-entry performance calculated by including the gravitational forces (solid lines) and the re-entry performance calculated by neglecting them (dotted lines). Graphs 13 and 16 indicate that, for values of $\pi > 0.2$, the light body approximation is sufficiently precise in the prediction of both the velocity distribution and the acceleration distribution. Concerning the largest deceleration occuring in flight, Fig. 19 shows that the light body approximation is also

sufficiently precise, provided the ballistic factor exceeds 0.2.

5.3.2. Ballistic Missile with Variable Geometry(*)

The maximum deceleration can be reduced considerably by employing a variable geometry configuration. For example, consider a missile equipped with spoilers, which are controllable in flight. In the hypervelocity regime, each position of the spoilers corresponds to a different drag coefficient and, therefore, to a different ballistic factor. Of particular interest is the case where the spoilers are continuously retracted according to the power law

$$K_\beta = \frac{K_{\beta 1}}{\sigma^x}$$

where $K_{\beta 1}$ is the ballistic factor at sea level and x a constant such that

$$0 < x < 1$$

In this case the mathematical model can be reduced to that used in the investigation of the constant geometry missile if the following transformation of coordinates is introduced

---

(*) This problem has been investigated by Miele and Cappellari (Ref. 4) for light missiles. The extension presented here is concerned with heavy ballistic missiles.

$$\pi = \frac{K_{\beta 1}}{1 - x}\,\sigma^{1-x}$$

$$\epsilon = \frac{u^2}{2}\,(1 - x)$$

In fact, it can be immediately verified that Eqs. (62-3) and (72) reduce to

$$\frac{d\epsilon}{d\pi} + \epsilon - \frac{1}{\pi} = 0$$

and

$$\alpha = \epsilon\pi - 1$$

Consequently, all the formulas developed for the constant geometry missile are simultaneously valid for the variable geometry missile, provided the constant C defined by Eq. (68) be replaced by

$$C = (1 - x)\left[\frac{u_1^2}{2} + \eta_1\right] - \gamma_E - \log\frac{K_{\beta 1}}{1 - x} \qquad (86)$$

Notice that the decelerations occuring in flight are approximately proportional to the constant C and that the kinetic energy term is predominant on the right-hand side of both Eqs. (68) and (86). Consequently, the following rule of thumb is deduced: the ratio r of the maximum deceleration occuring in a variable geometry missile to the maximum deceleration occuring in a constant geometry missile is approximately

$$r \cong 1 - x$$

As an example, the maximum deceleration occuring in a variable geometry missile such that $x = 0.4$, is about 60% of the maximum deceleration occuring in a constant geometry missile.

5.4. Skipping Paths(*)

A trajectory of interest for long range hypervelocity vehicles is the so-called skip trajectory, which is composed of an alternate succession of ballistic phases and skipping phases. In the ballistic phase the vehicle operates in a quasi-vacuum environment beyond the outer reach of the atmosphere. In the skipping phase the vehicle enters the atmosphere, negotiates a turn, and is ejected once more from the atmosphere.

Owing to the relatively short distance covered in the skipping phase (order of magnitude: 10^2 miles) the hypothesis of flat Earth is justified. Furthermore, since the aerodynamic forces are, on the average, much

---

(*) This problem has been previously investigated by Eggers, Allen, and Neice who derived Eqs. (91) and (92). The extension presented here is concerned with the analytical determination of the range and the distribution of normal, tangential, and total accelerations along a skipping path.

larger than the gravitational forces, a simple, though approximate, analysis can be carried out by simplifying Eqs. (45-3) and (45-4) as follows

$$\dot{u} + K_D u^2 \sigma = 0 \tag{87}$$

$$\dot{\gamma} - K_L u \sigma = 0 \tag{88}$$

The integration process for these equations and for the associated kinematic relationships is now carried out in connection with a path flown with constant angle of attack in the hypervelocity realm. This means that K_D, K_L, E are regarded to be constant.

Altitude. Eqs. (45-2) and (88) are now combined to give the following differential equation

$$K_L \, d\sigma + \sin\gamma \, d\gamma = 0 \tag{89}$$

whose general solution is

$$\sigma = \frac{1}{K_L} (C + \cos\gamma) \tag{90}$$

where C is a constant. Consequently,

$$\eta = \log \frac{K_L}{C + \cos\gamma} \tag{91}$$

It is evident from Eq. (91) that the non-dimensional altitude η is a single-valued function of the cosine of the path inclination. Therefore, if η_e is a conventional altitude designating the outer reach of the atmosphere

and if the initial and final conditions are assumed such that

$$\eta_i = \eta_f = \eta_o$$

one obtains

$$\gamma_f = -\gamma_i$$

Notice that the minimum altitude is obtained when $\gamma = 0$. Consequently, in order to avoid hitting the ground during the skipping phase, it is necessary that the lift factor be consistent with the inequality

$$K_L > 1 + C \cong 1 - \cos\gamma_i$$

Velocity. By combining the two dynamic relationships and eliminating the time, the following differential equation is obtained

$$\frac{du}{u} + \frac{d\gamma}{E} = 0$$

whose general solution is

$$u = C_1 \exp(-\frac{\gamma}{E}) \qquad (92)$$

as was predicted in Section 2.2. Consequently, the ratio of final velocity to initial velocity becomes

$$\frac{u_f}{u_i} = \exp(2\frac{\gamma_i}{E})$$

Since γ_i is negative, this equation clearly points out the importance of the lift to drag ratio if the skipping phase is to be performed with relatively low loss in kinetic energy.

Range. Eqs. (45-1), (88), and (90) lead to the following differential equation for the distance traveled

$$\frac{d\xi}{d\gamma} = \frac{\cos\gamma}{\cos\gamma + C}$$

whose general solution is

$$\xi = \gamma - \frac{C}{\sqrt{1 - C^2}} \log \left| \frac{\tan\left(\frac{\gamma}{2}\right) + \sqrt{\frac{1 + C}{1 - C}}}{\tan\left(\frac{\gamma}{2}\right) - \sqrt{\frac{1 + C}{1 - C}}} \right| + C_2 \tag{93}$$

where C_2 is a constant. Assuming

$$\frac{\sigma_i K_i}{\cos\gamma_i} << 1$$

the following approximations hold

$$\frac{C}{\sqrt{1 - C^2}} = \cot\gamma_i$$

$$\sqrt{\frac{1 + C}{1 - C}} = -(1 + \varphi)\tan\left(\frac{\gamma_i}{2}\right)$$

where

$$\varphi = \frac{K_1 \sigma_1}{\sin^2 \gamma_1}$$

Consequently, after taking $\xi_1 = 0$, Eq. (93) becomes

$$\xi = \gamma - \gamma_1 - \cot \gamma_1 \log \left| \frac{2 + \varphi}{\varphi} \frac{(1 + \varphi) \tan \frac{\gamma_1}{2} - \tan \frac{\gamma}{2}}{(1 + \varphi) \tan \frac{\gamma_1}{2} + \tan \frac{\gamma}{2}} \right| \tag{94}$$

This means that the total distance flown during the skipping phase becomes

$$\xi_f = -2 \left[\gamma_1 + \cot \gamma_1 \left(\eta_1 + \log \frac{2 \sin^2 \gamma_1}{K_1} \right) \right] \tag{95}$$

Discussion. Eqs. (91) and (94), which represent the geometry of the flight path, have been employed to calculate some typical skipping trajectories. In this connection, Fig. 22 illustrates the effect of the entrance angle on flight trajectories where $\eta_1 = 10$, $K_1 = 1$; on the other hand, Fig. 23 illustrates the effect of the lift factor for $\eta_1 = 10$ and $\gamma_1 = -20^\circ$. Both diagrams indicate that the range flown during the skipping phase decreases as the lift factor and the modulus of the entrance angle increase. This effect is clearly shown in Fig. 24, where the overall range is

plotted versus the entrance angle for $\eta_1 = 10$ and for several values of the lift factor.

Acceleration. Eqs. (91) and (93) indicate that the geometry of the skipping trajectory depends on the initial altitude, the entrance angle, and the lift factor. On the other hand, it is independent of the entrance velocity. Thus, as the entrance velocity increases, higher accelerations must be expected at all points of the flight path.

In order to compute the acceleration, it is convenient to define the following dimensionless parameters

$$\alpha_n = \frac{V}{g}\frac{d\gamma}{dt}$$

$$\alpha_t = -\frac{1}{g}\frac{dV}{dt} \qquad (96)$$

$$\alpha = \frac{1}{g}\sqrt{\left(\frac{dV}{dt}\right)^2 + \left(V\frac{d\gamma}{dt}\right)^2}$$

which are, respectively, proportional to the normal acceleration, the tangential deceleration, and the total acceleration. Notice that, because of the equations of motion

$$\alpha_n = K_L \sigma u^2$$

$$\alpha_t = K_D \sigma u^2 \qquad (97)$$

$$\alpha = \sqrt{K_L^2 + K_D^2}\ \sigma u^2$$

so that

$$\alpha_1 = \frac{\alpha_0}{E}$$

$$\alpha = \frac{\alpha_0}{E}\sqrt{E^2 + 1}$$

As a conclusion, the distributions of the tangential deceleration and total acceleration are proportional to the distribution of the normal acceleration, if the skipping phase is performed at constant angle of attack.

Concerning the normal acceleration, simple manipulations, omitted for the sake of brevity, lead to

$$\frac{\alpha_0}{u_1^3} \cong (\cos\gamma - \cos\gamma_1) \exp\left[\frac{2(\gamma_1 - \gamma)}{E}\right] \qquad (98)$$

where u_1 is the dimensionless entrance speed. This function attains a maximum during the descending branch of the flight trajectory. The associated path inclination must satisfy the following transcendental equation

$$\sin\gamma + \frac{2}{E}(\cos\gamma - \cos\gamma_1) = 0 \qquad (99)$$

whose solution is indicated in Fig. 25. The maximum values of the normal acceleration, the tangential deceleration, and the total acceleration are plotted in Figs. 26 through 28 versus the entrance angle and the lift to drag ratio.

The main conclusion to be derived from these diagrams is that the maximum acceleration increases very rapidly when the entrance velocity and the modulus of the entrance angle increase. Thus, accelerations in the order of 20-30 g are not impossible during the skipping phase, a rather negative circumstance from a structural standpoint and, for manned vehicles, from a physiological viewpoint.

Concerning the normal acceleration, Fig. 26 indicates that this component of the acceleration increases as the lift to drag ratio increases. Thus, the requirements of a low loss in kinetic energy and that of a low normal acceleration yield contrasting conclusions as far as the choice of the lift to drag ratio is concerned. This means that, in practice, a compromise value must be selected for E.

Another parameter of interest is the non-dimensional normal acceleration at the lowest point of the trajectory. The latter is supplied by

$$\frac{a_n}{u_1^2} = (1 - \cos\gamma_1) \exp\left(\frac{2\gamma_1}{E}\right) \qquad (100)$$

and is plotted in Fig. 29 for several values of the entrance angle and the lift to drag ratio. In turn, the tangential deceleration and the total acceleration are indicated in Figs. 30 and 31.

ACKNOWLEDGMENT

The writer is indebted to Messieurs David G. Hull, Arthur H. Lusty, and Robert E. Pritchard for their valuable assistance in connection with the preparation of this report.

CONCLUSIONS

A general analytical theory of the flight paths of a glider operating over a flat Earth is presented. First, the equations of motion are non-dimensionalized by introducing a set of variables which depend on one undetermined parameter, the reference velocity. Then, particular problems are analyzed; for each of these, a reference velocity which reduces the equations of motion to their simplest possible form is selected.

Three categories of problems are considered: (a) flight in an arbitrary atmosphere, (b) flight in a homogeneous atmosphere, and (c) flight in an exponential atmosphere. For each of these categories, a survey of previous research is made, and new analytical results are presented. It is shown that problems of type (a) cannot be solved analytically but that closed form solutions for problems of type (b) and (c) are possible in the low subsonic and hypervelocity regimes.

Particular attention is given to flight trajectories in an exponential atmosphere, such as shallow paths, vertical paths, re-entry paths, and skipping paths.

With regard to the re-entry of a heavy ballistic missile, analytical criteria are supplied in order to determine the points of maximum velocity and maximum deceleration. By employing a variable geometry configuration, the maximum deceleration can be reduced considerably, up to forty percent in a particular example.

For skipping paths, the point of maximum acceleration occurs during the descending portion of the flight trajectory. Although the maximum normal acceleration increases with the lift to drag ratio, the maximum tangential acceleration decreases. Consequently, the maximum total acceleration has a minimum with respect to the lift to drag ratio. For an entrance angle of twenty degrees, this minimum occurs for a lift to drag ratio of about one.

REFERENCES

1. ALLEN, H. J., and EGGERS, A. J., Jr., "A Study of the Motion and Aerodynamic Heating of Missiles Entering the Earth's Atmosphere at High Supersonic Airspeeds", NACA T.N. No. 4047, 1957.

2. EGGERS, A. J., Jr., ALLEN, H. J., and NEICE, S. E., "A Comparative Analysis of the Performance of Long-Range Hypervelocity Vehicles", NACA T.N. No. 4046, 1957.

3. LINNELL, R. D., "Vertical Re-entry into the Earth's Atmosphere for both Light and Heavy Bodies", Jet Propulsion, Vol. 28, No. 5, 1958.

4. MIELE, A., and CAPPELLARI, J. O., Jr., "Effect of Drag Modulation on the Maximum Deceleration Encountered by a Re-entering Ballistic Missile", Purdue University, School of Aeronautical Engineering, Report No. A-59-6, 1959.

5. NATIONAL BUREAU OF STANDARDS, "Tables of Sine, Cosine, and Exponential Integrals", Vols. I and II, 1940.

6. TEMPLIN, R. J., and CALLAN, M. M., "Generalized Trajectory Curves for Bodies Moving in Air", National Aeronautical Establishment of Canada, Laboratory Report LR-159, 1956.

7. MALINA, F. J., and SMITH, A. M. O., "Flight Analyses of a Sounding Rocket", Journal of the Aeronautical Sciences, Vol. 5, No. 5, 1938.

8. TURNACLIFF, R. D., and HARTNETT, J. P., "Generalized Trajectories for Free-Falling Bodies of High Drag", Jet Propulsion, Vol. 28, No. 4, 1958.

9. KATZEN, E. D., "Terminal Phase of Satellite Entry into the Earth's Atmosphere", Jet Propulsion, Vol. 29, No. 2, 1959.

10. SÄNGER, E., and BREDT, J., "A Rocket Drive for Long Range Bombers", Bureau of Aeronautics, Navy Dept., Translation No. CGD-32, 1944.

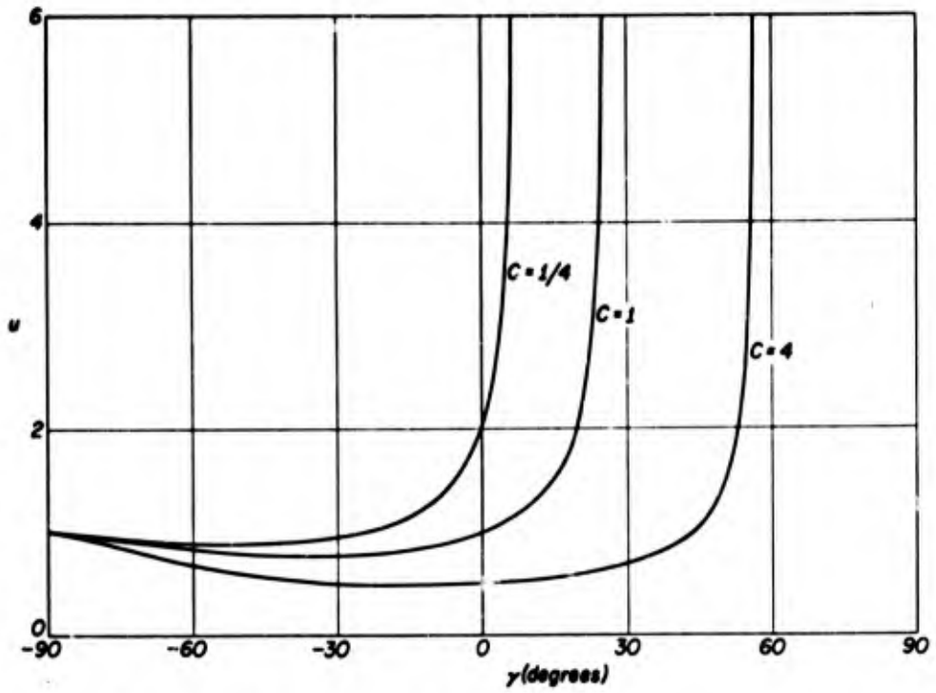

Fig. 1. Relationship between velocity and path inclination (zero lift, homogeneous atmosphere).

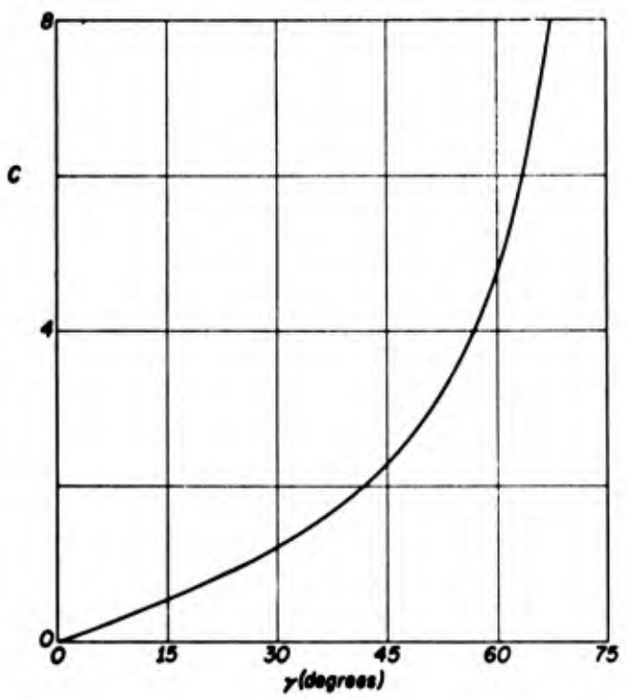

Fig. 2. Asymptotic value of the path inclination (zero lift, homogeneous atmosphere).

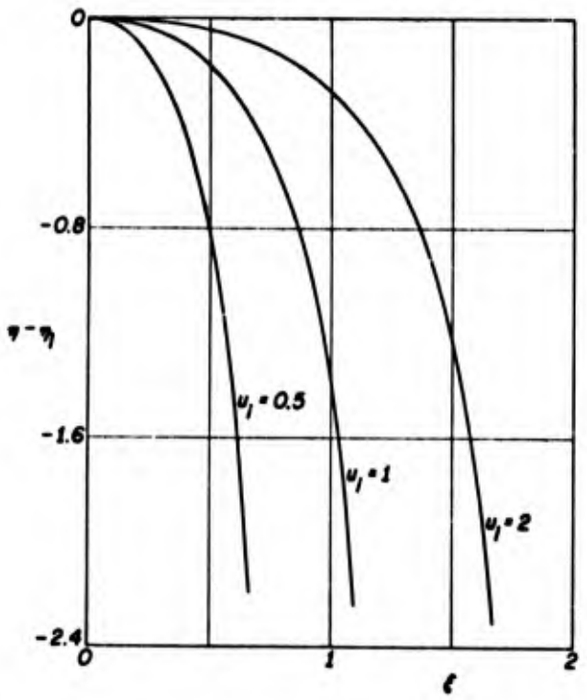

Fig. 3. Geometry of the flight path (zero lift, homogeneous atmosphere).

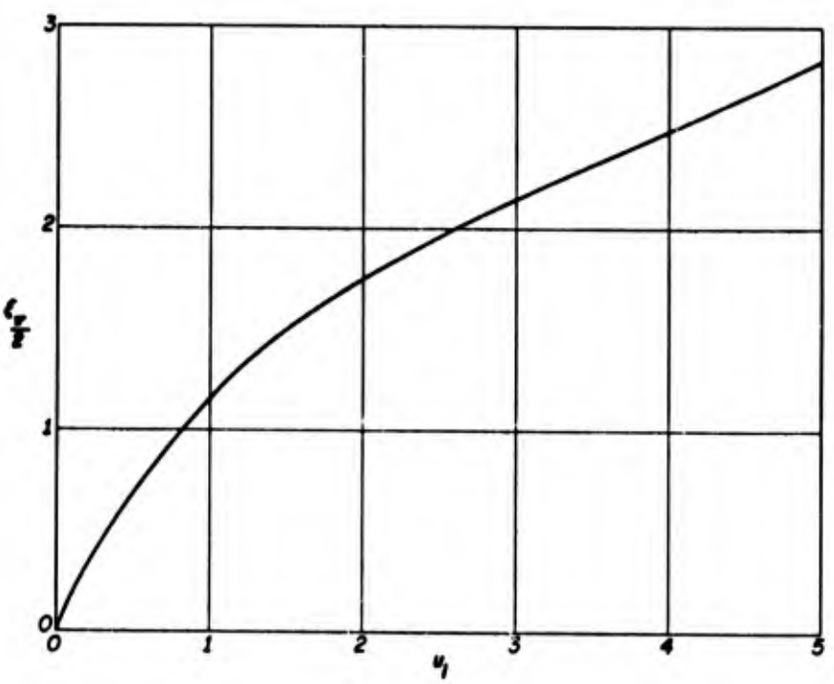

Fig. 4. Limiting distance traveled by an object launched horizontally (zero lift, homogeneous atmosphere).

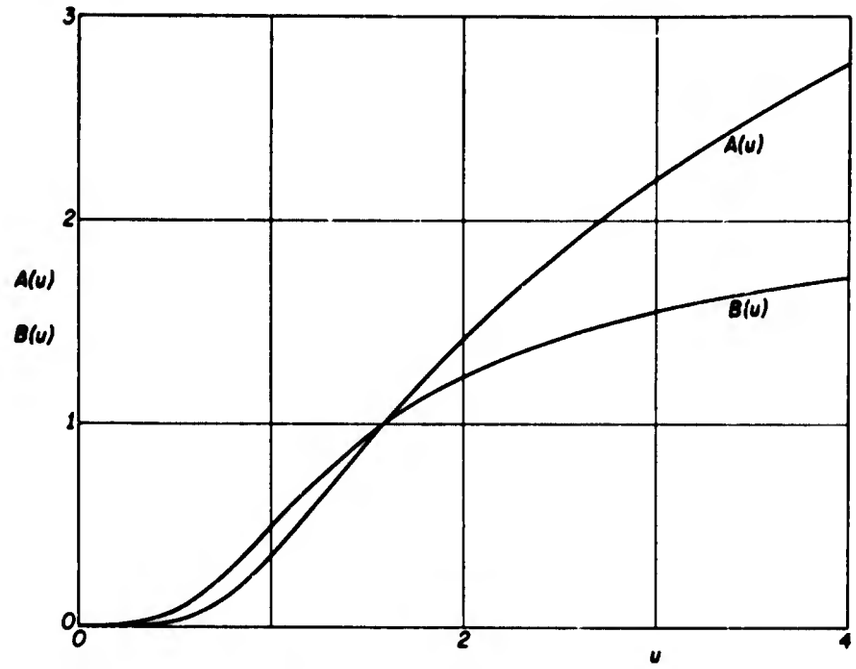

Fig. 5. The functions A(u) and B(u).

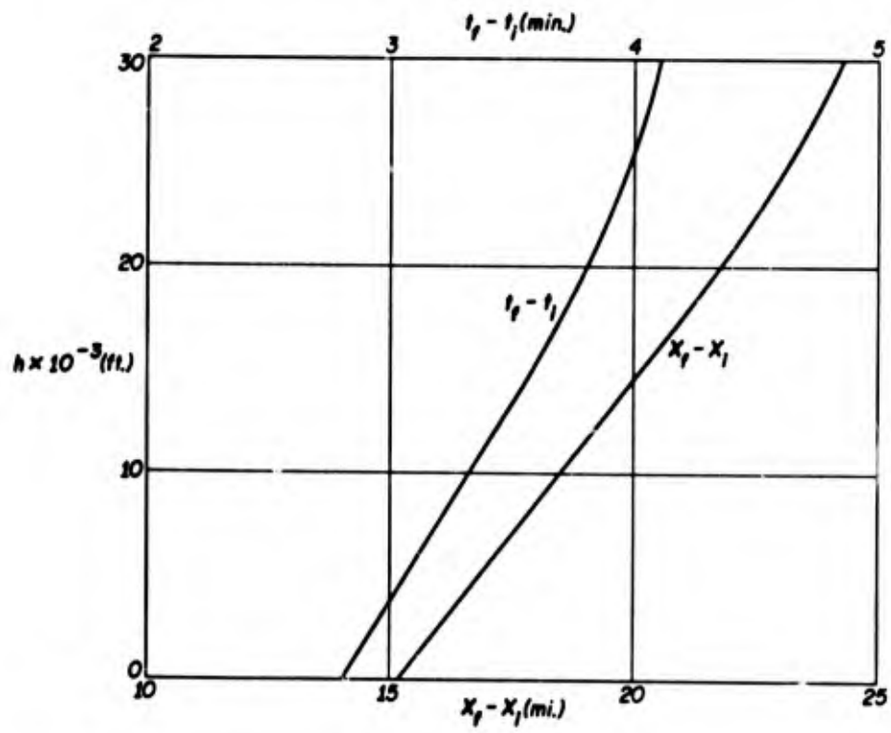

Fig. 6. Level flight deceleration distance and deceleration time of a typical jet transport at different altitudes.

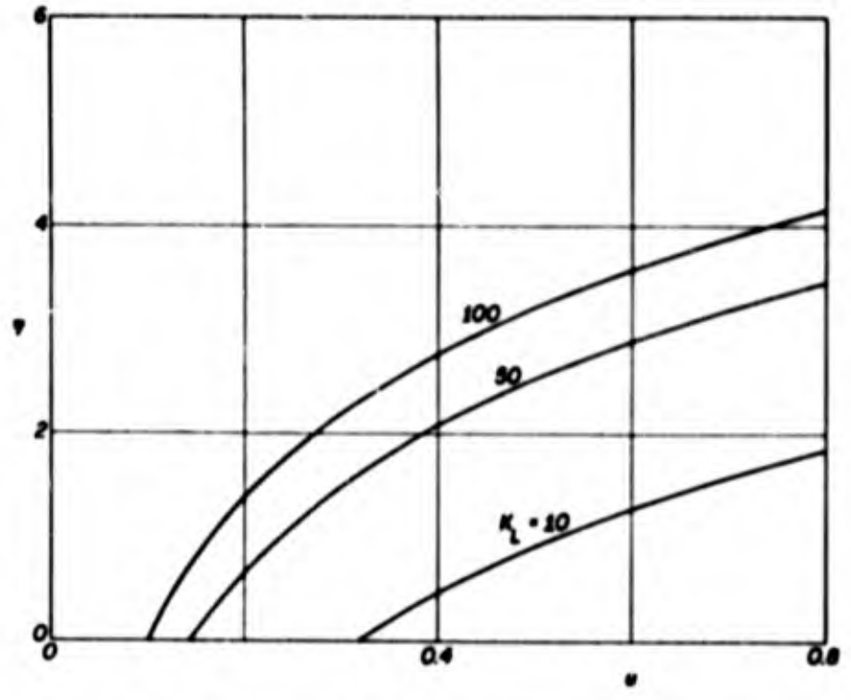

Fig. 7. Relationship between flight altitude, instantaneous velocity, and lift factor for a shallow path.

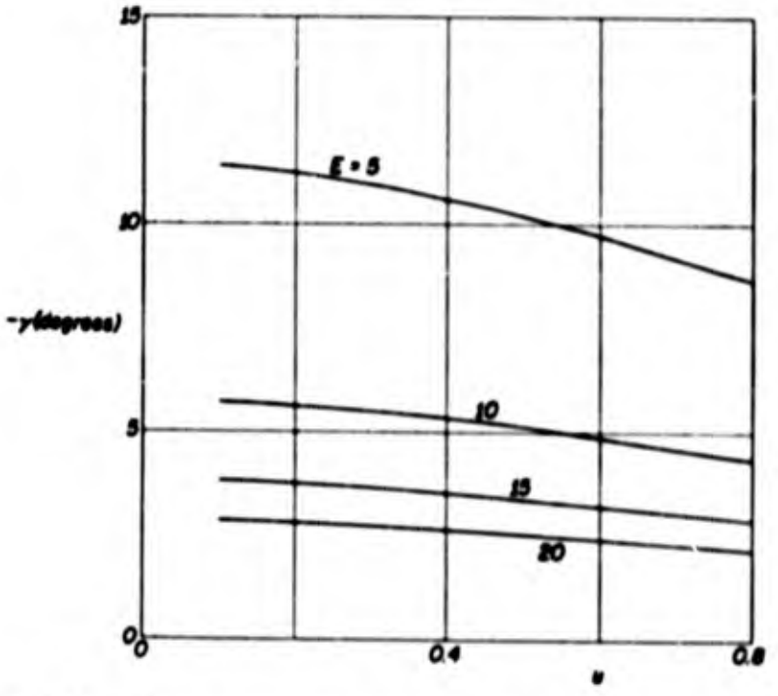

Fig. 8. Relationship between path inclination, instantaneous velocity, and lift to drag ratio for a shallow path.

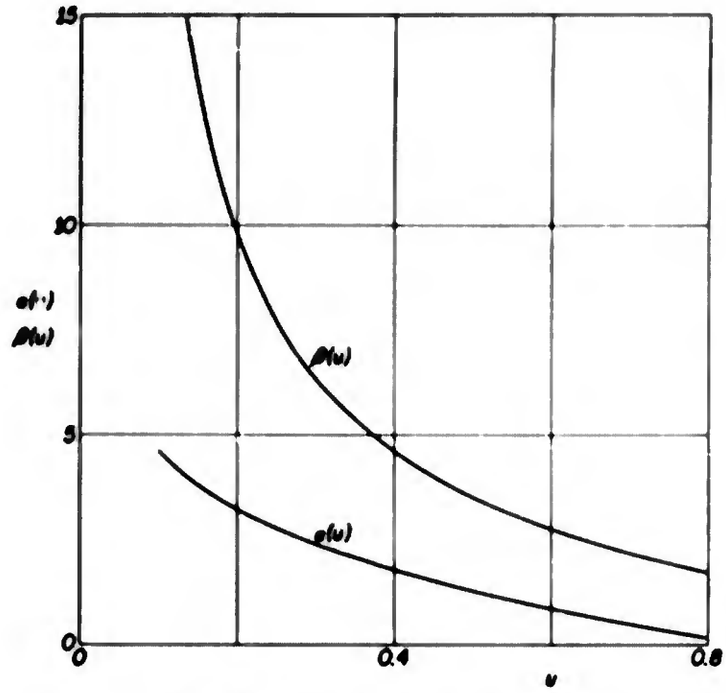

Fig. 9. The functions $\alpha(u)$ and $\beta(u)$.

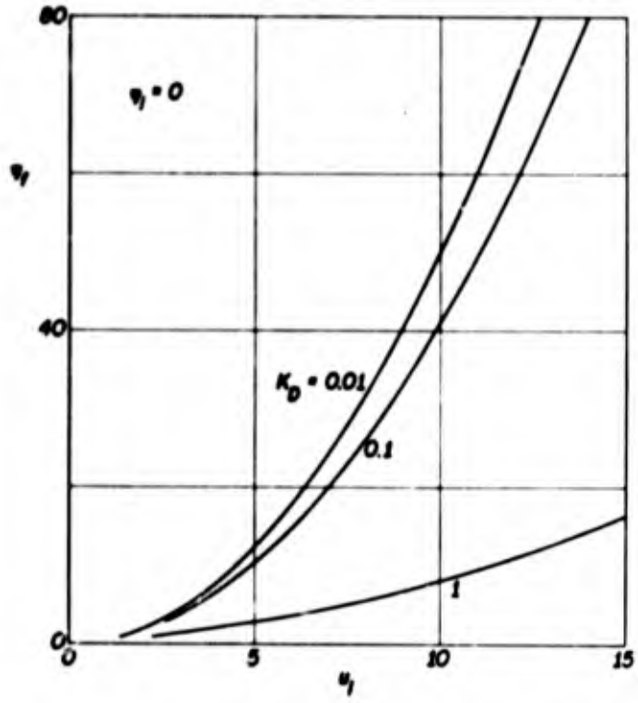

Fig. 10. Peak altitude reached by a sounding rocket versus initial velocity and drag factor.

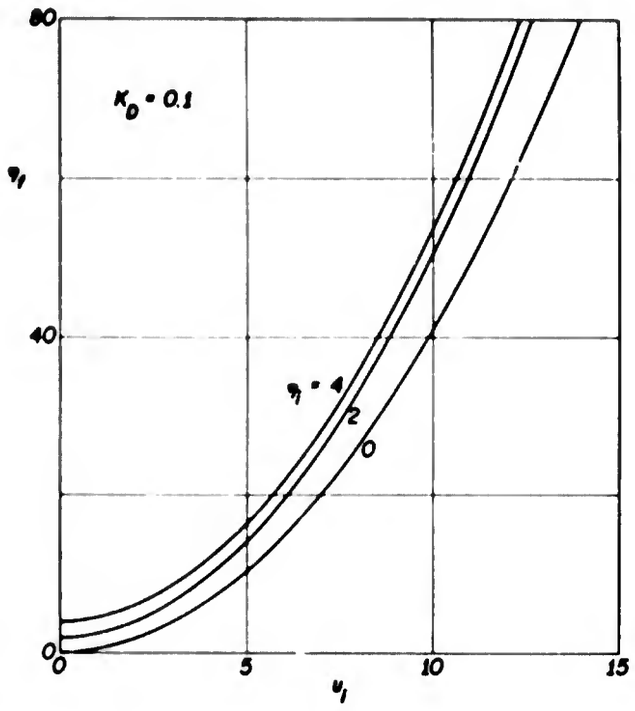

Fig. 11. Peak altitude reached by a sounding rocket versus initial velocity and initial altitude.

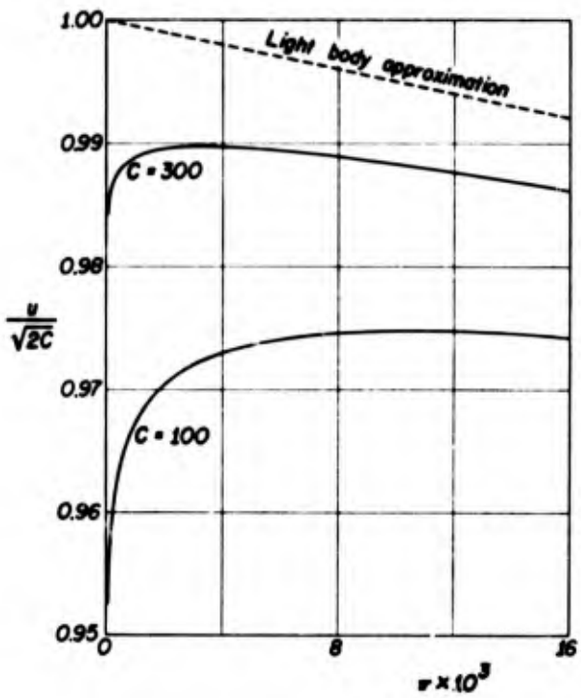

Fig. 12. Velocity distribution along a re-entry path.

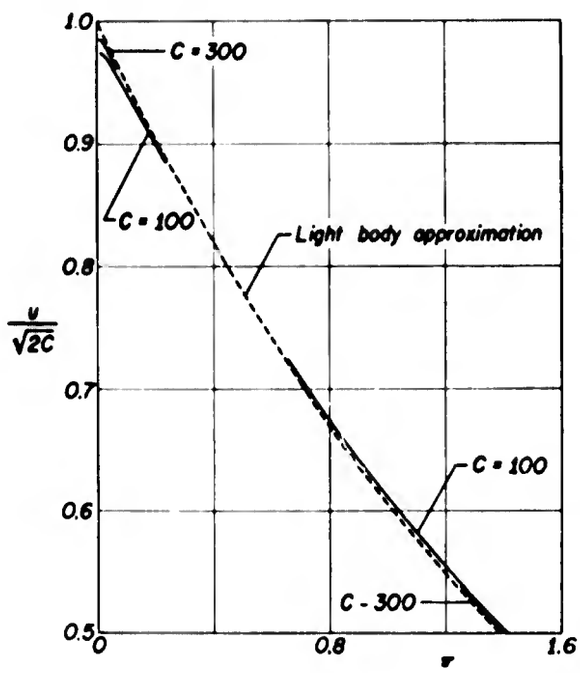

Fig. 13. Velocity distribution along a re-entry path.

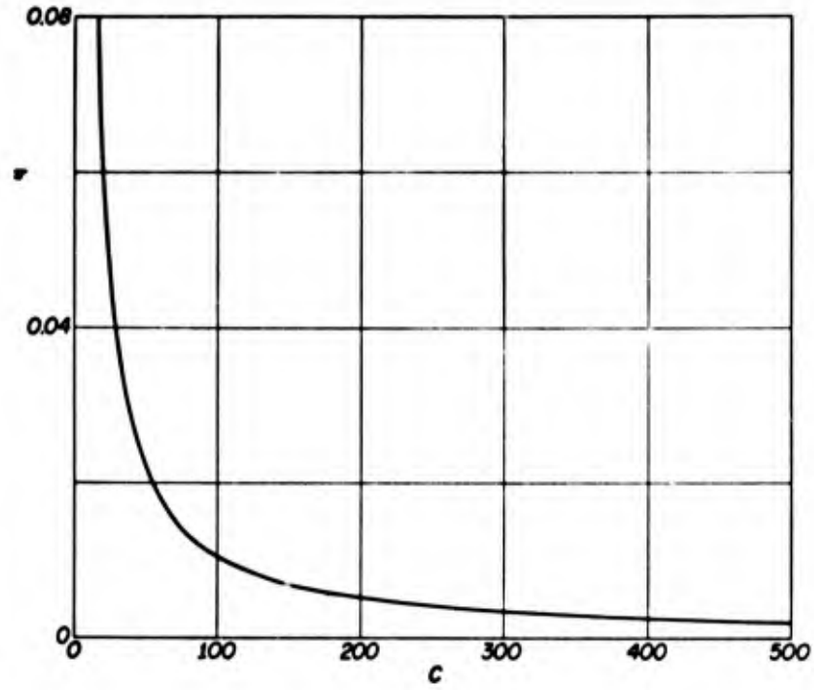

Fig. 14. Maximum velocity point in a re-entry path.

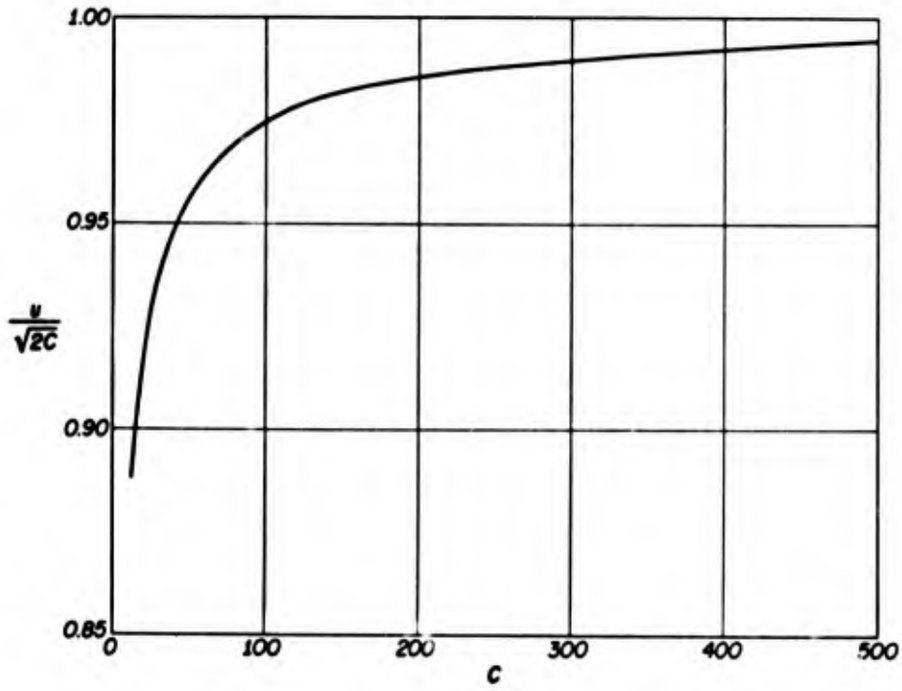

Fig. 15. Maximum velocity in a re-entry path.

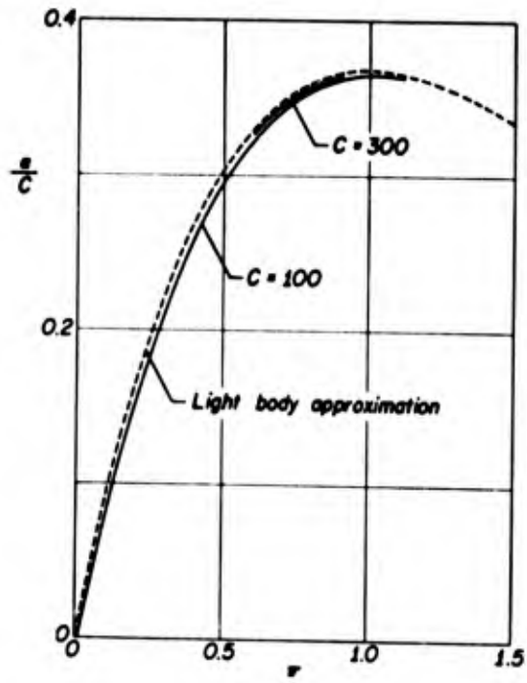

Fig. 16. Distribution of decelerations along a re-entry path.

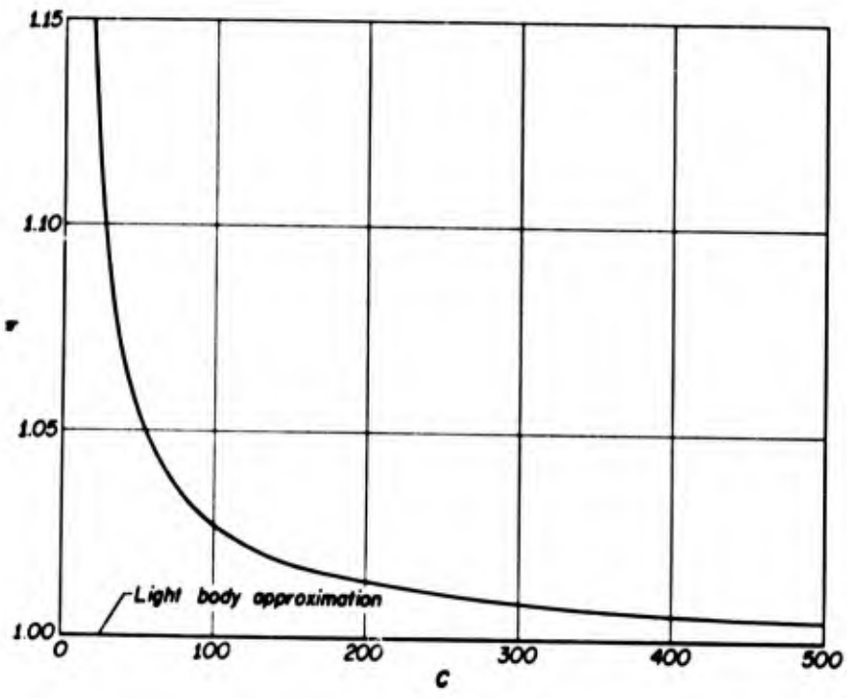

Fig. 17. Maximum deceleration point in a re-entry path.

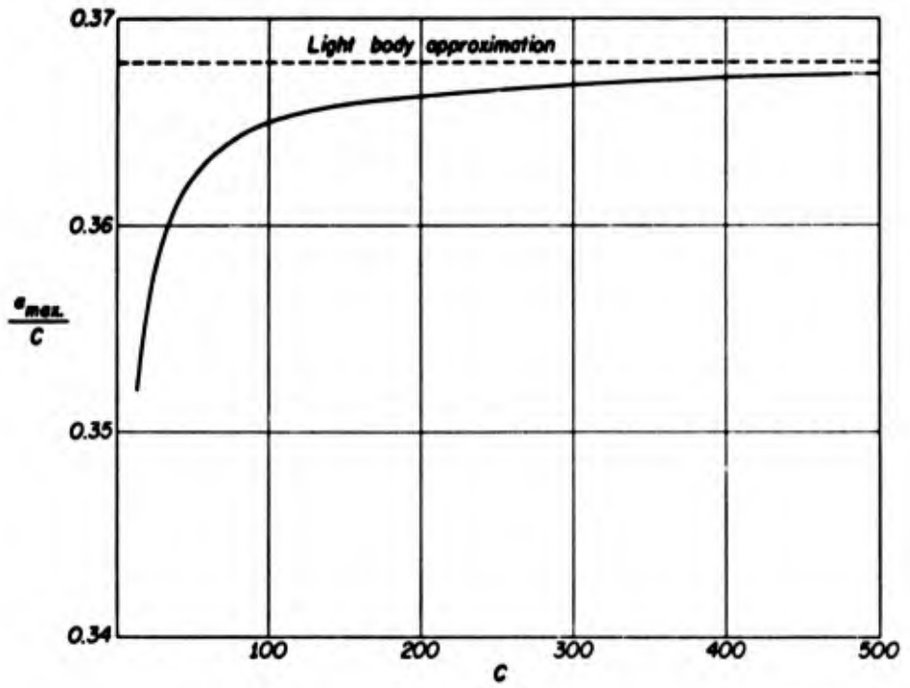

Fig. 18. Maximum deceleration in a re-entry path.

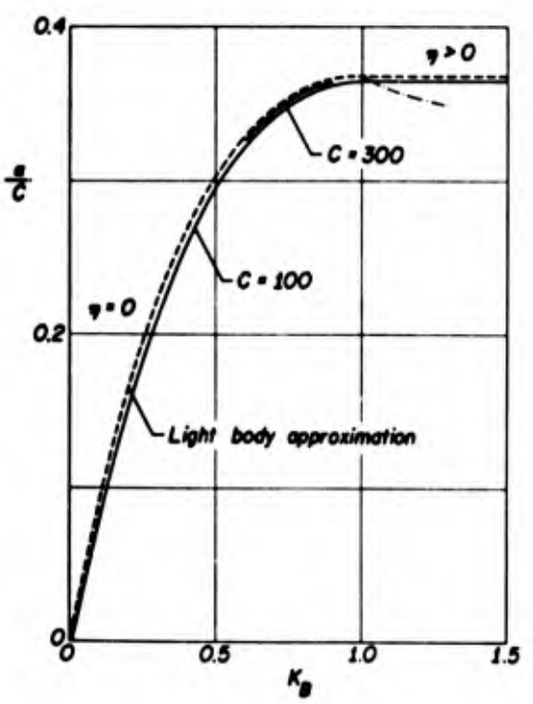

Fig. 19. Envelope of the largest decelerations occuring in a re-entry path.

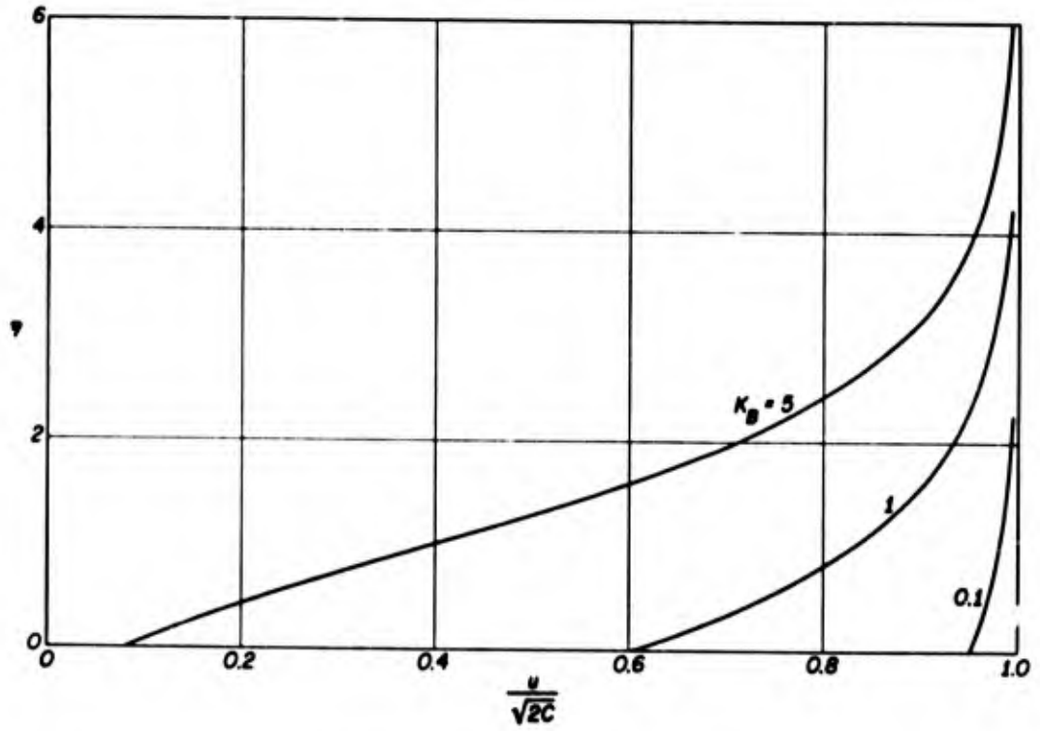

Fig. 20. Velocity-altitude diagram along a re-entry path for several values of the ballistic factor (light body approximation).

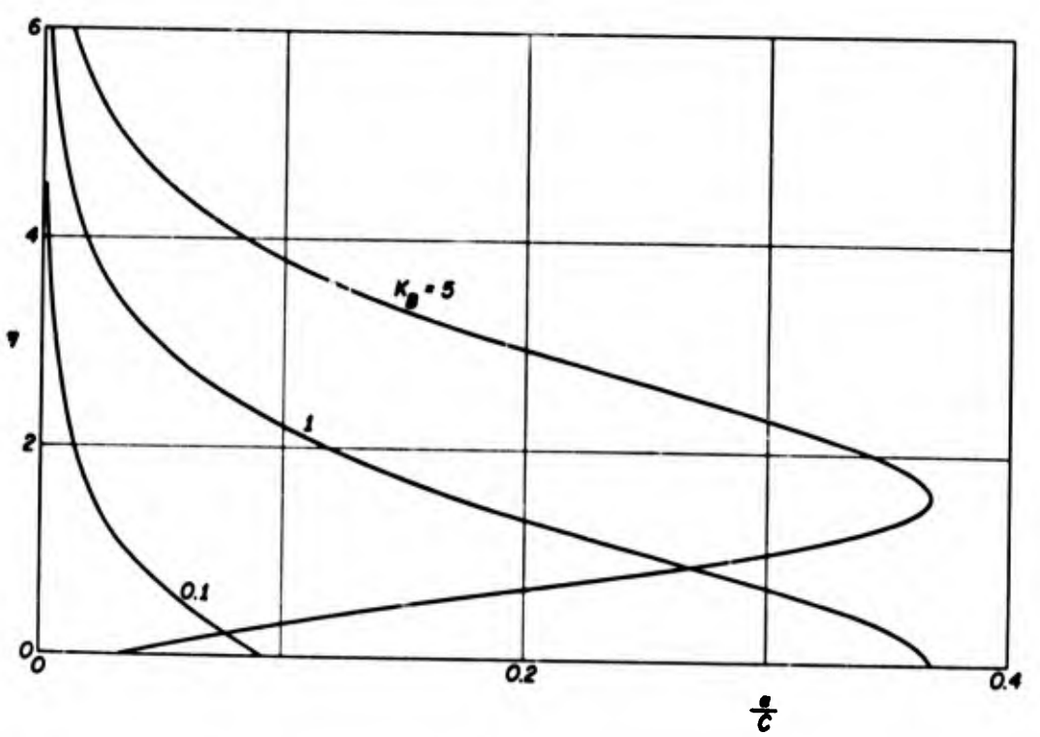

Fig. 21. Deceleration-altitude diagram along a re-entry path for several values of the ballistic factor (light body approximation).

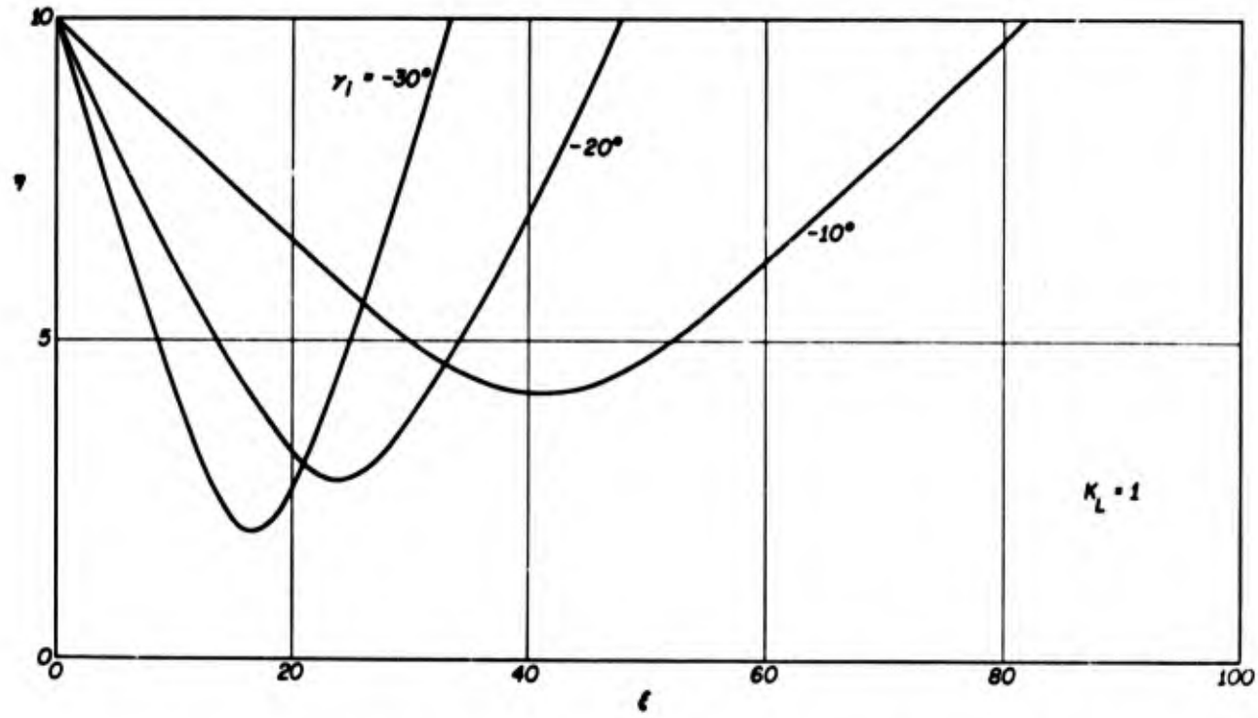

Fig. 22. Effect of the entrance angle on the geometry of a skipping path.

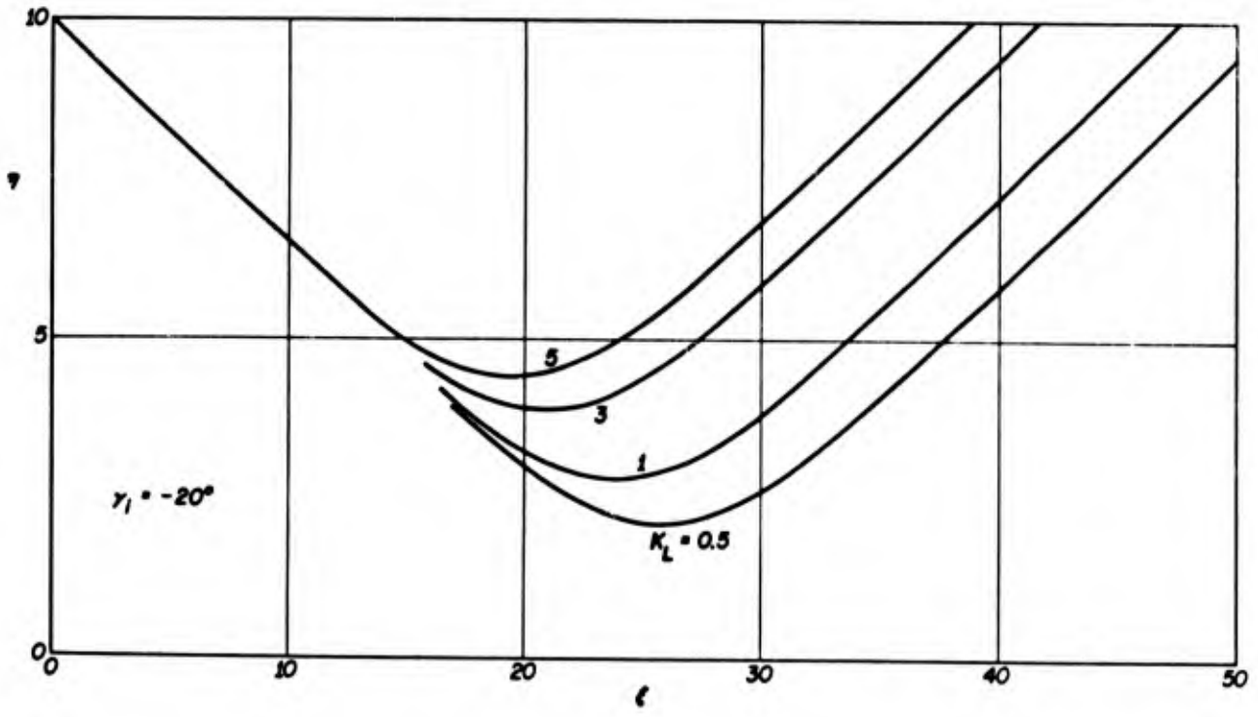

Fig. 23. Effect of the lift factor on the geometry of a skipping path.

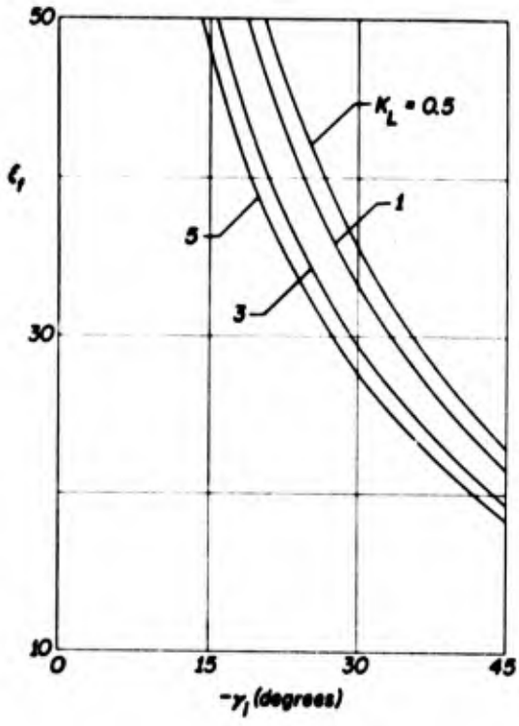

Fig. 24. Effect of the entrance angle and the lift factor on the overall range flown during the skipping phase.

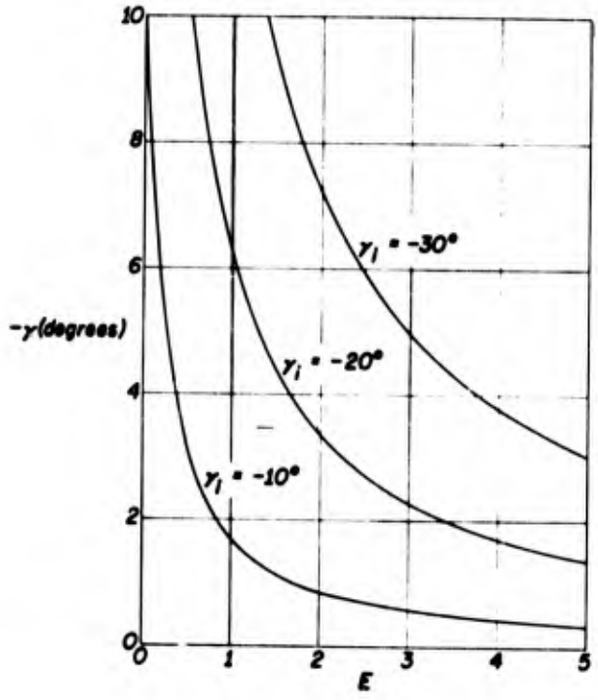

Fig. 25. Maximum acceleration point in a skipping path.

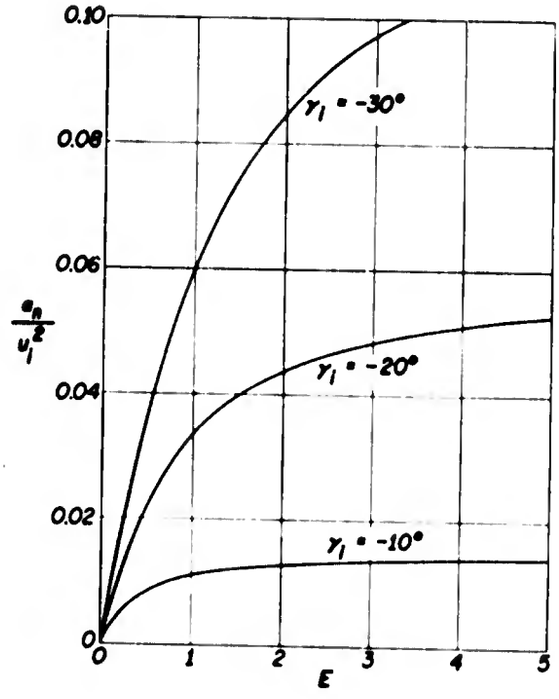

Fig. 26. Maximum normal acceleration in a skipping path.

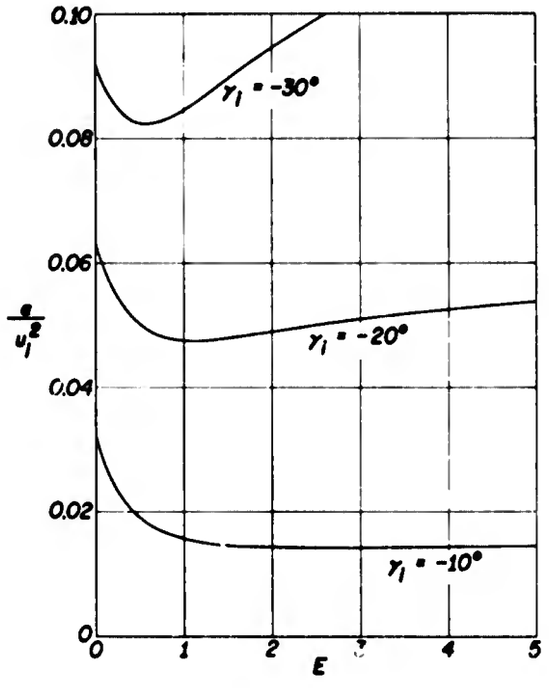

Fig. 27. Maximum tangential deceleration in a skipping path.

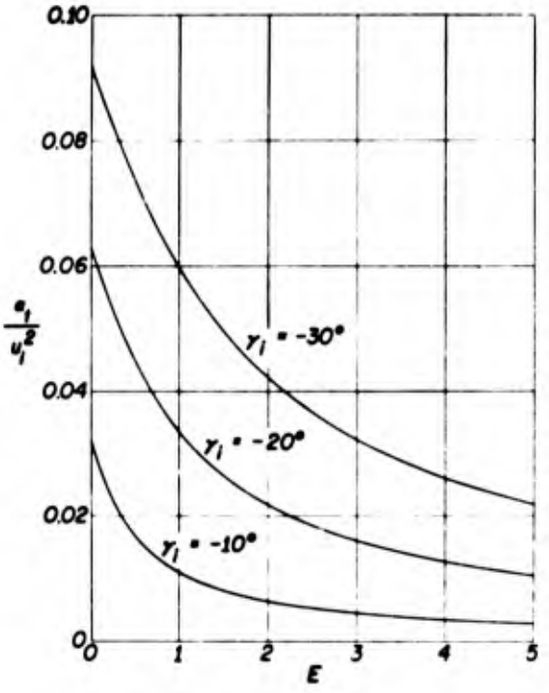

Fig. 28. Maximum total acceleration in a skipping path.

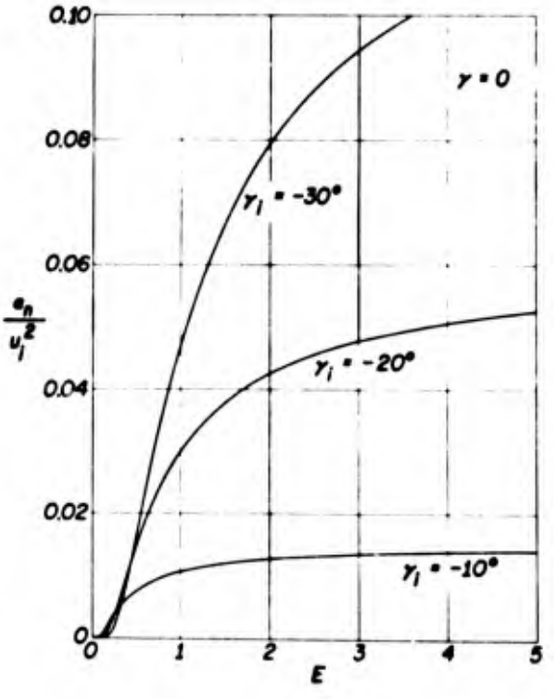

Fig. 29. Normal acceleration at the lowest point of a skipping path.

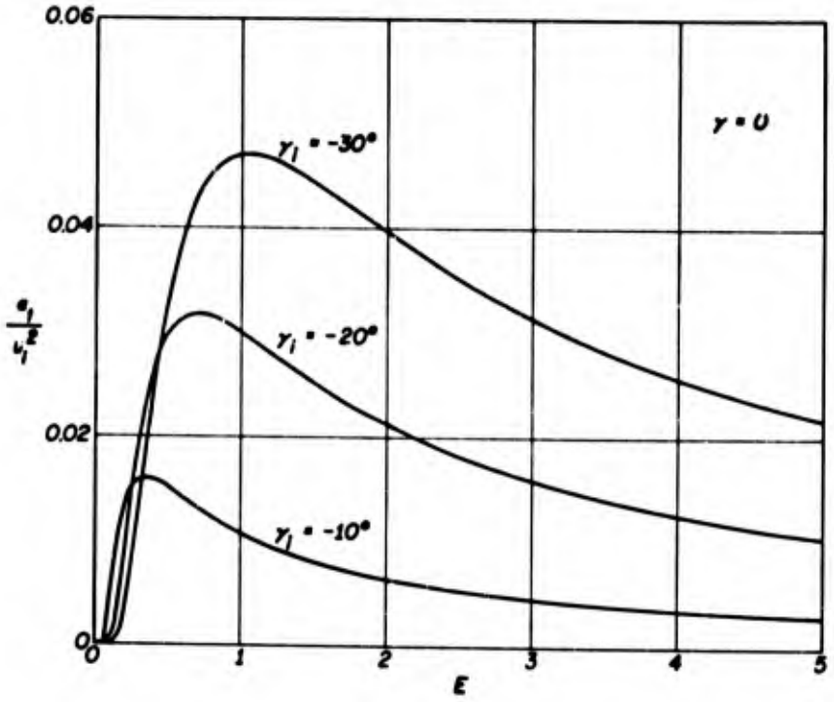

Fig. 30. Tangential deceleration at the lowest point of a skipping path.

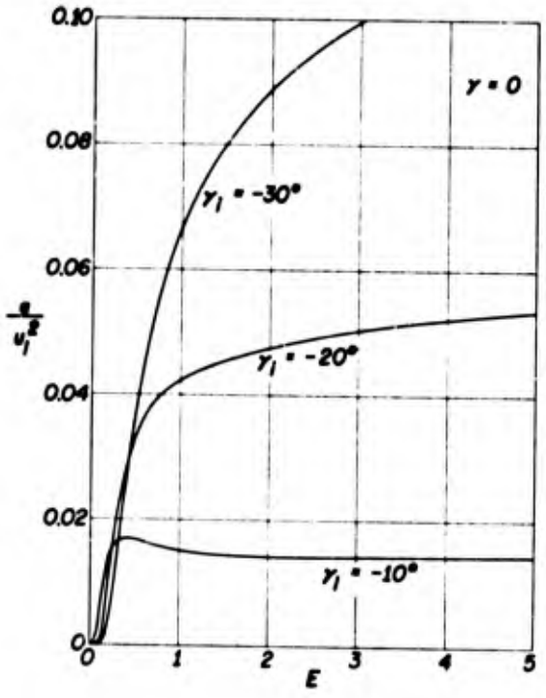

Fig. 31. Total acceleration at the lowest point of a skipping path.